DEVELOPMENT OF A TRIBOELECTRIC NANOGENERATOR USING NYLON-HYBRID YARN

Karnasooriya Ragalage Sanjaya Dinuwan Gunawardhana

(198014T)

Thesis Submitted in Partial Fulfilment of The Requirements for the Degree Master of Science by Research

Department of Textile and Apparel Engineering

University of Moratuwa
Sri Lanka

February 2021

Declaration

I K.R.S.D. Gunawardhana (198014T) declare that this is my own work, and this thesis does not incorporate without acknowledgement any material previously submitted for a Degree or Diploma in any other University or institute of higher learning and to the best of my knowledge and belief it does not contain any material previously published or written by another person except where the acknowledgement is made in the text. Also, I hereby grant to University of Moratuwa the non-exclusive right to reproduce and distribute my thesis/dissertation, in whole or in part in print, electronic or other medium. I retain the right to use this content in whole or part in future works (such as articles or books).

Signature: Date:

The above candidate has carried out research for the Master by Research thesis/ dissertation under my supervision.

Signature of the supervisor: Date:

Dedication

සුවහසක් දුක් විඳ මා ඇති දැඩි කල අම්මාටත්

කටට ලේ රස එන තුරු දරුවන්ට සිප් කිරි පොවමින් මා පෝෂණය කල

තාත්තාටත්

වරදට දඬුවම් දෙමින් සුපෙක්ශල ලෙස මා ඇස් පෑදූ ගුරු දෙමව්පියන්ටත්

ආදරය ශක්තියක් වෙමින් සැමදා ලඟින් සිටි අසංකා ඔබටත්

මෙය උපහාරයක් වේවා.....

let this be a tribute to

my mother

my father

my teachers

and my love....

Acknowledgement

First and foremost, I would like to express our sincere gratitude to my Master of Science by a major component of the research Project Supervisor, Dr.N. D. Wanasakara, to present the initial idea to initiate this research and his continuous support and guidance throughout the entire project. I highly appreciate his devoted efforts in formulating the necessary background, connecting me with the resources, and correcting my mistakes.

My sincere gratitude goes to Dr T.S.S.Jayawardhana, Research Coordinator of the Department of Textile and Apparel Engineering, coordinates the progress reviews, supports other necessities, and guides us throughout the project. Moreover, my heartiest gratitude goes to Prof. (Mrs.) U.G.S. Wijayapala, Head of Department of Textile and Clothing Technology, provided me with the necessary guidance and facilities in implementing the project successfully. I especially need to express gratitude to all the lab in charge and other academic staff for helping me with the problems that arise with enlightening me regarding the activities corresponding to the research project and throughout this period.

Furthermore, my profound gratitude goes to Dr Ishara Dharmasana, Doctoral Research Fellow, Loughborough University, who taught me the essence of Triboelectric Nanogenerators' field and introduced this technology to Sri Lanka. In addition to that, the support he gave me with material sourcing and electrical result characterization while giving vital feedback throughout the project execution period helps me improve the project's standards and eliminate possible future mistakes.

I want to express my gratitude to prof. S.U. Adhikari, senior lecturer Department of Materials Science Engineering for being the external investigator for the first and second progress review. His guidance was beneficial to do the project on the correct path.

This research's financial support was provided through the SRC Grant (SRC/ST/2019/24) offered by the Senate Research Council, University of Moratuwa. I want to extend my sincere thanks to SRC to identify this research's value and approve the short-term grant to cover some expenses related to the project.

Moreover, my sincere gratitude goes to Mr Malaka Perera and Mr Rajitha Botheju, Technology Entrepreneur at MAS holdings, for material sourcing and technical support at the project's initial and final stage.

Finally, I would like to express my heartiest gratitude towards my family, anyone, and everyone who supports me to achieve great success at the completion and their kind co-operation and encouragement, which helped me complete this project.

Abstract

Human needs are continually changing with the enhancement of novel electronic technologies. The Internet of Things (IoT), Artificial Intelligence, and 5G technology have led to state-of-the-art products to improve the living standards if a rapidly increasing global population. Wearable electronics, which closely associated with human activities, are typically powered with replaceable or rechargeable batteries. There are significant drawbacks of existing power supplies for wearable electronics, including low flexibility and stretchability, limited autonomy, low biocompatibility and high weight. Portable and renewable energy harvesting are possible from a wearer's physical movements in an ambient environment. In recent years, this has been achieved using Piezoelectric and Triboelectric nanogenerators, which act as an alternative to batteries for powering wearable electronic devices. However, such technologies' challenges include the magnitude and consistency of power output, fabrication for mass-scale production and operation under small mechanical movements. This project focus on developing a triboelectric nanogenerator using silver-coated nylon yarn, silicone and polyurethane with a rib knitting structure. The basic fundamental methods of applying triboelectric layers such as dip coating, printing and yarn coating methods analysis for wearable and electrical outputs. Yarn coated sample shows the best results with even coverage, good air permeability (101 cm3/cm2/s), high moisture management properties and high stretchability (Stretchability -75.82%, Recoverability- 76.67% and elastic modulus of 1.4093). Furthermore, when polyurethane bonded air textured sample used as a secondary triboelectric layer, the final device shows a maximum short circuit current of 3.412 $\mu A/m^2$, the charge density of 6.12 µC/m2 and maximum open-circuit voltage of 51.08 V under the 1 mm amplitude over 1 Hz frequency. Finally, the device used to generate a peak power of 116.8 µW/m2 through 10 GΩ resistors under the same motion profile.

Key Words: Triboelectric Nanogenerator, Wearable Energy Harvesting. Knitting, Air Texturing

Table of Content

List of Figures

List of Tables

List of Abbreviations

Abbreviation	Definition
3.5G	Gauge three point five
5G	Gauge Five
7G	Gauge seven
AATCC	American Association of Textile Chemists and Colourists
AC	Alternative Current
ASTM	American Standards of Testing Materials
BS	British Standards
CNT	Carbon Nanotube
DDEF	Distance Dependent Electric Field
EDAX	Energy dispersive X-ray Analysis
FSTENG	Freestanding Mode Triboelectric Nanogenerator
ISC	Short Circuit Current
JSC	Short Circuit Current Density
LSTENG	Lateral Sliding Mode Triboelectric Nanogenerator
PDMS	Polydimethylsiloxane
PET	Polyethylene Terephthalate
PLA	Polylactic Acid
PTFE	Polytetrafluorethylene
PU	Polyurethane
PVDF	Polyvinylidene Difluoride

PZT	Lead Zirconate Titanate
RTV	Room Temperature Vulcanized
SEM	Scanning Electron Microscope
SETENG	Single Electrode Triboelectric Nanogenerator
TENG	Triboelectric Nanogenerator
VCSTENG	Vertical Contact Separation Mode Triboelectric Nanogenerator
VOC	Open Circuit Voltage

CHAPTER 1

1. INTRODUCTION

1.1. Background to The Study

More than yesterday, human needs are evolutionarily changed with the enhancement of technology, and energy is becoming a critical factor in determining the efficiency and effectiveness of todays and future world technological developments. Internet of Things (IoT), 5^{th} generation technology, and Artificial intelligent are revolutionary technologies developing with the enhancement of wearable electronic devices[1]. A rapid expansion of the areas such as communication, security, healthcare, personal electronics, and sports have achieved significant quality over the life of the people globally[2]. Wearable electronic devices, being closely related to human activities, are powered with replaceable or rechargeable batteries that have encountered some significant drawbacks: low flexibility, low stretchability, less autonomy, low biocompatibility, and high weight. This not only disturbs the continuous operation but also increases the weight and toxicity while degrading flexibility, stretchability and other wearable characteristics[2]. Hence, there is an urgent demand for the development of efficient and sustainable power generation units for wearable electronics, which can make them self-powered for indefinite amounts of time without compromising wearable performance.

1.2. Research Problem

Energy harvesting from the ambient environment via technologies like Piezoelectric, Triboelectric, Photovoltaic and, Thermoelectric energy harvesting techniques are becoming much popular in the last few years as an alternative to replaceable or rechargeable batteries to power the wearable electronic device. Photovoltaic energy harvesting devices harness energy from sunlight or other light sources. The release of free electrons from the semiconductor materials or unique, organic dye materials under sunlight's irradiation creates the electron flow in photovoltaic nanogenerators[3]. On the other hand, Piezoelectric energy harvesting is first introduced back in 2006 by Z. L. Wang's group. The specific piezoelectric materials: lead zirconate titanate (PZT), Zinc Oxide (ZnO), can be electrically polarized under a strain-induced over system. Since textile materials are conformal materials, the load transferred to the piezoelectric material could be minimal to derive a sustainable power output[1].

Even though there are drawbacks to mechanical energy harvesting, human movements can be associated with energy harvesting devices, and many researchers are focusing on that area. Among other mechanical energy harvesting techniques, triboelectric nanogenerator (TENG) has attracted significant attention for mechanical energy harvesting, recording remarkable power outputs 900 V, 19 μA by 9 x 5 cm^2 surface area[4], and efficiencies exceeding 80%, as per recent literature[1]. Due to this high power and high converting efficiency, these devices can be triggered under minimal contact or separation, which suits textile-related applications. In the past, macro-and micro-scale energy harvesting solutions based on TENG have been developed[2], with flexible solutions for wearable architectures. Interestingly, many textile polymers listed in the triboelectric series, and many fabric architectures are suitable for efficient wearable TENG structures. Specifically, from a textile engineering perspective, knitted-fabric TENG devices show great potential with higher output performance due to high stretchability, flexibility and ease of fabrication[5]–[7]

However, there has been little progress in developing systematic approaches for, innovative textile-based fabric type TENG devices. By considering these factors, this MSc research project focus on creating a wearable TENG device using available textile engineering concepts such as knitting, printing, yarn coating and air texturing to achieve higher wearable and electrical performances. It is a taking step to covert lab-scale TENG devices to mass-scale production. In the first phase of this project, the feasibility analysis of selected triboelectric materials will be carried out to develop an optimized TENG device. The best triboelectric layer fabrication method will be selected based on bespoke electrical characterization mechanism and standard textile testing methods. Finally, as given in the topic and objectives, a TENG device will be prepared with enhanced charge collection using air texturing technique as a solution for wearable high power generated TENG development.

1.3. Significance of The Project

Wearable electronics sensors and devices have achieved drastic development throughout the last decade. After developing energy harvesting techniques, scientists worldwide are trying to overcome many issues related to powering those electronic devices. This project significantly exploits some prior knowledge about wearable TENG fabrication. The electrical and wearable performance of the triboelectric layer deposition techniques such as dip coating, printing and yarn coating has systematically analyzed for the betterment of this research avenue. Furthermore, textile engineering concepts such as Rib knitting, air texturing, Stenter process, and screen printing have used to optimize wearable TENG devices' characteristics.

Most of the wearable performance analyses are carried out according to the standards developed by American Standards of Testing Materials (ASTM), British Standards (BS) and the American Association of Textile Chemists and Colorists (AATCC). The use of standard test methods enhances the repeatability of the results in the future event of scaling up the mere TENG prototype into a commercialized product.

Moreover, the materials used in this project are readily available and can be used without further chemical enhancement or purification. Finally, the project's electrical characterization was carried out with Wolfson School of Mechanical, Electrical and Manufacturing Engineering at the University of Loughborough. They are working in TENG optimization using the theoretical model for the last few years and have published several rigorous peer review articles. That validates the accuracy of the electrical characterization with precise equipment.

1.4. Aim and Objectives of The Study

1.4.1. Aim

To systematically develop triboelectric nanogenerator with optimized wearable and electrical characteristics.

1.4.2 Research objectives

1. Identify and evaluate the potential materials to generate triboelectricity.
2. Assess the feasibility of printing, dip coating and yarn coating methods to develop triboelectric nanogenerators.

3. Develop and evaluate the samples for textile and electrical performance and compare the results to select the best mechanism.
4. Incorporate air texturing mechanism to conductive yarn and assess the changes over textile and electrical performance.

CHAPTER 2

2. LITERATURE REVIEW

2.1. Introduction to The Chapter

This chapter started with the operating principle of the TENG and its significance over other energy harvesting techniques. The chapter eventually extended towards micro and macro scale nanogenerators, wearable TENG evaluation. Finally, the research question is structured according to the literature and theoretical model-based optimization tools for TENGs.

2.2. Operation Principle and Working Mechanism Of TENG.

For thousands of years, the world experiences the triboelectric effect in different ways. From 2012 to the present, various research groups have conducted much research in micro and macro energy harvesting using TENGs. Low manufacturing cost, easy maintenance and fabrication, flexibility and scalability are becoming causes of the popularity of triboelectric nanogenerators in energy harvesting applications[2], [8]–[10].

TENG operation principle is mainly developed based on the triboelectric effect of the materials listed in the triboelectric series and the electrostatic induction between triboelectric material and the respective electrodes[1], [2]. Typically, TENG (Figure 2.1a) was constructed using two distinct materials in the triboelectric series, which placed opposite each other. The ability of a material to be charged with triboelectric effect with respect to a second reference surface is the base of constructing the triboelectric series (Figure 2.1b). The materials tend to be positively charged, are listed towards the top, while the materials, which tend to be negatively charged, are listed relatively lower in the series.

Interestingly, the triboelectric series contains many polymers and materials commonly used in textile applications[11], signalling the potential of using existing textile material systems for TENG applications [12]. The transfer of charge can be happening in the form of electrons, ions with a charge, nanoparticle, or a combination of all of this[1]. Two electrodes are connected to the top and bottom triboelectric layer to create the respective circuit. According to the place where the material lies in the triboelectric series, and many other structural parameters define the maximum power that can be harvested through the respective device[13].

Embedding TENG into textiles can be achieved in several ways. There are four main working modes in TENGs. Vertical contact separation mode (VCSTENG) (Figure 2.1c) is the most common operating mode of TENG, and most of the researches show that this has the capability of producing higher output[2]. The structure made with two triboelectric surfaces faces each other while electrodes are connected to one triboelectric material's top surface and the other triboelectric material's bottom surface. With the contact and separation of two triboelectric surfaces, a potential difference is created and that allows the flow of electrons from one electrode to another, creating an alternative current (AC)[9], [14].In most cases, textile-based TENG uses this operation mechanism because it can be easily embedded into two fabric layers with contact and separation natural movement[9].

The lateral sliding mode (LSTENG) (Figure 2.1d) charge separation mechanism is the same as the VCSTENG. The lateral movement of two triboelectric layers creates a potential difference, and due to that, electrons flow from one electrode to the other through the load resistor. Through rotation of a disk[15], movement of two planes [16] and cylindrical spins [17] energy can be harvested in this method. In textile-based TENGs use the linear grating structure to produce higher output using this mechanism[9].

Single electrode mode (SETENG) (Figure 2.1e) used when there is a possibility to ground the electrode through a reference load. Once the electrode is ground with a reference load resister, by contact separation or lateral movement triboelectric surface over the electrode, energy can be harvested. Compared with other methods, this method is not considered popular because of low output power [2]. This method can quickly produce energy just by a touch of hand or fabric[9]. Free-standing triboelectric layer mode (FSTENG) (Figure 2.1f) is a method used of two electrodes and one triboelectric layer. Two electrodes have placed one next to each other. By contact separation or lateral movement of the triboelectric layer over the electrodes can produce a current in between two electrodes. Primarily this mode can be used as a barrier for shielding effect[2].

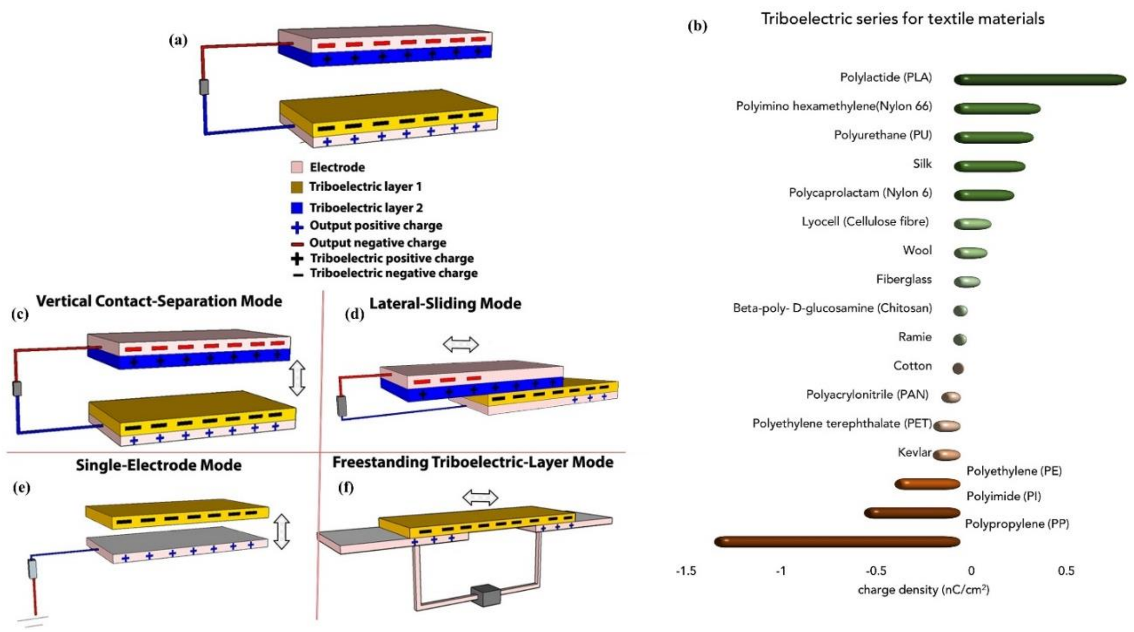

Figure 2.1: Working modes and triboelectric series for TENG devices, a) Common TENG Architecture, b) Triboelectric Series for Textile Material Adopted from [11], c) VCSTENG Mode TENG Architecture, d) LSTENG Mode TENG Architecture, e) SETENG Mode TENG Architecture, f) FSTENG Mode TENG Architecture

Source: reprinted with permission from ref [1], copyright The Authors.

Improvement of TENG to generate high power output can be achieved using several parameters. The selection of material is a critical factor in the case to generate high power output. It is advisable to select material further apart in the triboelectric series to generate the maximum output under minimum force. According to Dharmasana et al., by increasing the charge density, the power output can be increased quadratically while load resistance is set to optimum resistance (at optimum resistance, maximum power can be extracted from TENG)[18]. This results that greater attention needed to be given to enhance the charge density for efficient power generation. Even though there are conductive materials in the triboelectric series, it is impossible to use two conductive materials as the TENG device's triboelectric layers. To maintain voltage difference and specific stability over the power output, at least one of the triboelectric layers needed to be made out of insulating material while other conductive contact surfaces can act as the electrode and triboelectric layer.

2.3. Wearable TENG Development

Textile polymers such as Cotton[19], [20], Nylon[21], Silk[22], polyester[23] has used as the triboelectric substrate for TENG development in various ways. Furthermore, some novel polymers such as Polyethylene Terephthalate (PET)[24], [25], Chitosan[26], Polylactic Acid(PLA)[27], polyurethane (PU), and carbon fibres has achieved significant attention towards TENG development. Most of the TENG developments have used additional triboelectric materials such as polydimethylsiloxane (PDMS)[28], [29], Silicon rubber[30],Polytetrafluorethylene(PTFE)[20], [31], Polyvinylidene Difluoride (PVDF)[32] and perylene[33] in the form of printed, dip-coated, bonded or sticking layers over electrodes. Furthermore, since most of the textile materials are insulators, the electrode of wearable TENG devices is mostly developed using graphene-based materials such as carbon nanotubes[34], Metals or metal nano particles[35], [36] and polyaniline[37]. These electrode materials have used in the form of yarns, nano-fibre membranes, wires or surface coatings to enhance the surface area.

Textiles-based TENG devices in literature can be categorized under three main categories; Fibre, Yarn or Fabric-based TENG devices. Since TENG devices are still developing, most of the devices are yet to be progressed towards the mass scale with production parameters. Fibre or yarn-based TENG developments can be mainly categorized in the form of core-sheath structures (Figure 2.2a) and sandwich structures (Figure 2.2b). These developments are carried out in the form of fibre or yarn twisting techniques[38], [39], coiling or wrapping sheath around core using motor[40], [41], electrospinning over an electrode surface[42]. These developed fibres or yarns can be embedded into textile fabrics using weaving(hand loom[43], shuttle loom[44]), Knitting[28], sewing and embroidery[45], [46] methods.

Core sheath model-based TENG devices can work in VCSTENG, LSTENG and most popularly in SETENG. While working in the mode of SETENG, human skin can be considered a secondary triboelectric layer for such devices. More importantly, the core-sheath structures typically used the conductive material as the core, while triboelectric material as the sheath prevents leakage of induced electrons in the core electrode[31], [34]. Other than power generation, these devices can be used as self-powered sensing devices.

Sandwich structure-based TENG devices are mainly developed using nano-fibre membranes. Nanofibers made out of electrospinning process or any other fibre extrusion technique are sandwich in-between two conductive layers is the basic architecture of these kinds of devices. The use of nano-fibres enhances the surface area of the triboelectric surface, thus improving the charge density. Moreover, these TENG devices exhibit many wearable characteristics, such as air permeability and drapability, since there are enough spaces between nano-fibres. Some fibre and yarn-based TENG devices found in the literature are given in Table 2.1.

Table 2.1: Summary of Selected Sandwich and Core-Sheath Based TENG Devices Available in the Literature.

Year	Construction	Remarks	Output
2017 [34] (Figure 2.2b)	Silicon rubber coated with Carbon nanotube (CNT), again covered with silicone and copper microwire wrapped	For sensing applications	VOC* - 140 V ISC**- 0.18 mA/cm Charge density - 6.1 nC/cm. Power - 5.5 mW through 320 MΩ load, stretch2 Hz frequency
2018 [32]	Silk fibroin and PVDF nanofibres	Electrospun over two conductive surfaces to act as a hybrid nanogenerator	VOC - 500 V ISC - 12 mA Power density - 310 mW/cm^2 through 100 MΩresistor under hand tapping at 2 Hz frequency
2019 [47]	Nonwoven polypropylene and nylon 6,6	Nonwoven layers sandwiched between Ni coated fabrics	VOC - 210 V JSC***- 28.3 mA/m^2, Charge density - 97.3 nC power density - 901.7 mW/m^2 through 70 MΩ resistors with 6-Hz frequency contact separation movement.

2020 [41] (Figure 2.2a)	Silk and PTFE wrapped around stainless-steel core	Shuttle loom and embroidery technique	VOC- 45 V JSC -0.2 mA/m^2 Power – 3.5 mW/m^2 Through 50 MΩ under contact separation of 2 Hz
2020 [48]	PVDF, polyacrylonitrile electrospinning over silver yarn	Woven array for sensing application	VOC - 40.8 V ISC - 0.705 mA/cm Charge density - 9.513 nC/cm^2 using 5N force under 2 Hz frequency
2020 [42]	Carbon nanofibres sandwiched between PVDF nanofibres and PU nanofibres	PVDF acquire negative charge by contact with skin.	power density - 85.4 mW/m^2 through 50 MΩ resistor using 140 kPa pressure. sensitivity - 0.18 V/kPa the range between 0 and 175 kPa

Source :[32], [34], [41], [42], [47], [48] , VOC* - open circuit voltage, ISC** - short circuit current, JSC***- Short circuit current density,

More than fibre or yarn-based TENG developments, Fabric-based TENG developments are prominent with wearable energy harvesting related applications. Easy fabrication: Easy functionalization with chemical and mechanical methods and easy handling are the leading cause to make this method's more popular method among TENG development. In this method, the fabric must be used as either a Triboelectric layer, Substrate for electrode or Electrode. Even though some fabric-based TENG devices exhibit outstanding electrical performance, achieving wearable and aesthetic performance is challenging since the fabric-based TENG developments are achieved using dyeing, spin coating, dip coating, or screen printing[1], [9]. Furthermore, surface enhancement can be achieved using electrodeposition, Plasma treatment, Reactive ion etching or Lithography techniques (Figure 2.2c).

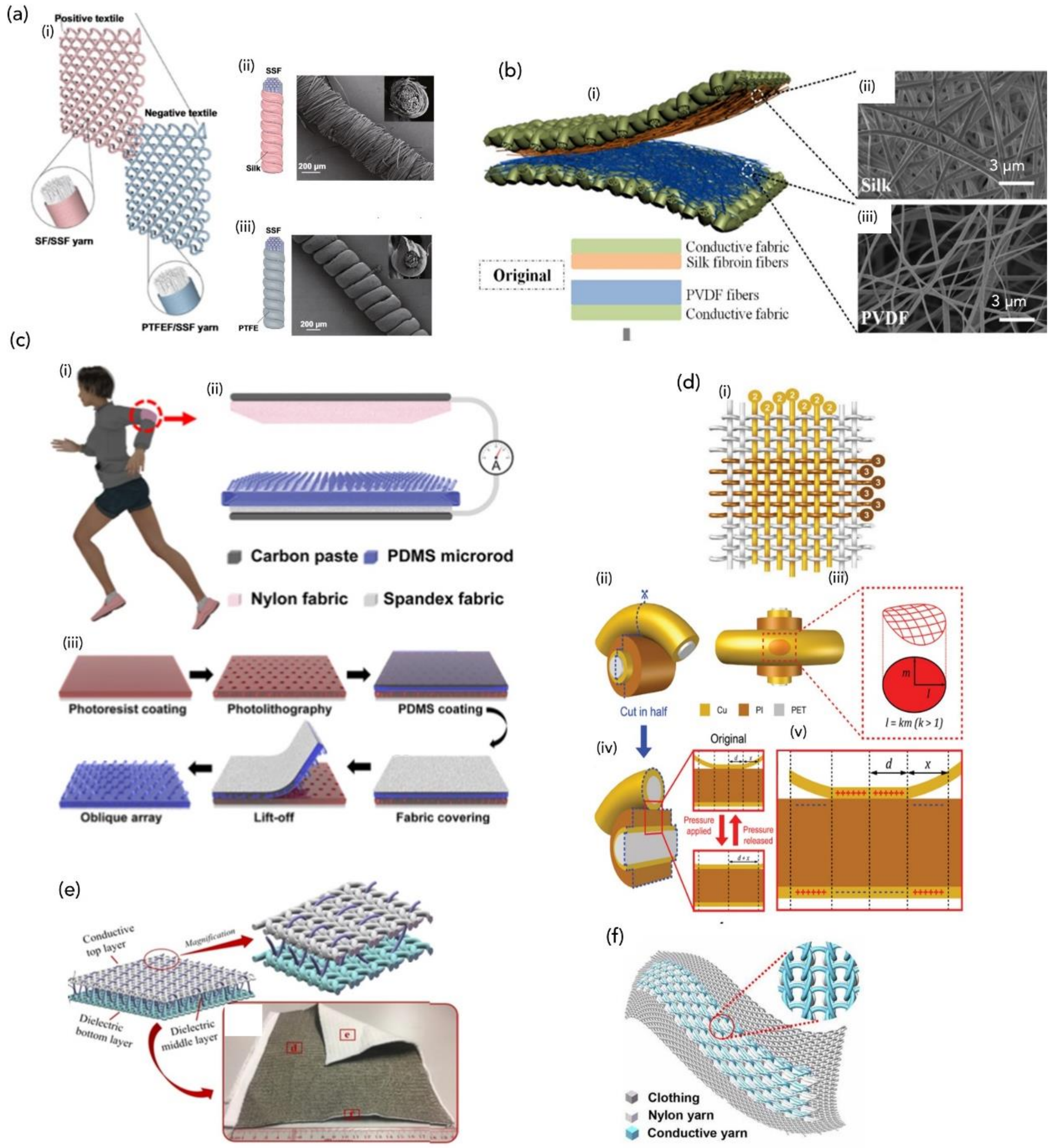

Figure 2.2: fibre/yarn, fabric based TENG devices, a) Silk/ Stainless Steel and PTFE/Stainless Steel Core-Sheath Based TENG Device. SEM Images for (ii) Silk/ Stainless Steel and (iii) PTFE/Stainless Steel. (b) (i) Piezoelectric and Triboelectric Hybrid Nanogenerator Constructed Using sandwich structure. SEM Images of (ii) Silk Nanofibers and (iii) PVDF Nanofibers., c) TENG Architecture of Harnessing Energy from Mechanical Movement, (ii) Schematic of Fabric Substrate-based TENG (iii) PDMS Microrods on Fabric., d) (i) Copper PET Yarn-based Woven TENG, Yarn Interlacing View from Side (ii) and Top (iii), (iv) Cross-sectional View of the Interlacing Point Under Pressure (Top) and Without Stress (Bottom), (v) Charge Distribution at Yarn Interlacing Point. (e) Schematic of 3D Knitted TENG Device, f) Full Cardigan Structure-based TENG Architecture

Source : (a) Reprinted from ref [49], b) Reprinted from ref [32], c) Reprinted from ref [50], d) Reprinted from ref [25],e) Reprinted from ref [51], f) Reprinted from ref [52]

Fabric-based TENG devices can be designed in woven (Figure 2.2c, d), knitted (Figure 2.2e, f) or a combination of different techniques. Among these woven fabric-related, TENG development is the most common method, and those devices can be functionalized in the forms of surface modification or structural modification. Woven fabrics are used as substrates for nano or micro-scale surface modifications which applied using chemical or mechanical methods in the case to improve the contact area with higher charge density[24], [36], [53]. Even though earlier developments are mostly used VCSTENG, LSTENG mode, and2- or 3-layer fabric substrates, the recent products are more focused on 3D woven structured based single devices.

Table 2.2: Summary of Selected Knitted and Woven Based TENG Devices Available in the Literature.

Year	**Construction**	**Remarks**	**Output**
2015 [54]	Al nanoparticles were grown over AU coated fabric electrode. Bottom made with PDMS	Woven structured Spin coating and reactive ion etching used for modification	VOC - 368 V ISC - 78 mA power density - 33.6 mW/cm^2 through a 20 Ω load, using 20 mm/s frequency 3 cm amplitude
2019 [50] (Figure 2.2c)	Carbon printed over Nylon woven fabric. PDMS micro rods over Spandex fabric	Reactive ion etching to create carbon nanowires. PDMS micro rods using lithography	VOC - 1,014.2 V JSC - 3.24 mA/cm^2 Charge density - 10.28nC/cm^2 power density of 211.7 mW/cm2 through a 6 MΩ load with 5 Hz frequency and 10 mm amplitude

2019 [25] (Figure 2.2d)	Cu/PET yarn as warp and polyamide coated CU/PET as weft	Using shuttle weaving technique	VOC - 4.98 V JSC - 15.50 mA/m^2 Power density - 33.16 mW/m2 through 60 MΩ underhand tapping
2019 [4]	Ag coated nylon separated by cotton. PTFE membrane attached to the polyester	Free-standing triboelectric layer mode based Knitted TENG device	VOC - 900 V ISC - 19 mA, Power - 203 mW/m^2 through 80 MΩ resistor
2019 [51] (Figure 2.2f)	Ag coated nylon for top and polyacrylonitrile based yarn as the bottom	3D knitted spacer fabric structure	Power density - 1,768.2 mW/m^2 through a 50 MΩresistor contact force of 1200 N
2020 [52] (Figure 2.2e)	Stainless steel/terylene twisted yarn for negative layer nylon yarn plated for positive	Full cardigan knit structure used. nylon yarns tucked alternatively	Pressure sensitivity 0-4 kPa - 7.84 mV/Pa 4 kPa < - 0.31 mV/Pa

Source [4], [25], [50]–[52], [54]

On the other hand, knitted fabric based TENG devices exhibits excellent mechanical characteristics like higher stretchability, drapability and breathability (unless surface coated or covered). Knitted fabrics are developed using three basic stitch types known as a knit stitch, tuck stitch, and miss stitch. Moreover, using techniques such as jacquard, interloping patters, and intarsia, TENG devices can be incorporated into different portions of a given fabric made of knitting. The majority of available TENG devices are developed using weft knitting structures since the individual controls different needles to perform unique structural advancements[7]. Among weft knitted structures, rib gating has proven with higher output along with higher stretchability[6]. Some woven and knitted fabric based TENG devices found in the literature are summarized in Table 2.2.

2.4. Electrical and Wearable Output Enhancement

Optimization of TENG devices is mostly achieved through understanding the theoretical behaviour of triboelectrification and electrostatic induction. According to maxwell's displacement current theory, the electrostatic induction is governed by the electric field variation around the electrodes used. Which controls the AC flow through the electrode under mechanical movement or deformation. By considering the TENG construction factors such as the thickness of the triboelectric layer, the TENG surface area, the separation between triboelectric layers, the permittivity of the triboelectric layer material, scientists developed relationships between the Voltage, Charge and Current output generation. The parallel plate capacitor approximation method and Distance dependence electric field method (DDEF) are two prominent theoretical models developed recently regarding TENG optimization. In parallel plate approximation, a relationship was built between Voltage (V), Charge (C) and TENG layer separation (X).

$$V = -\frac{Q}{S\varepsilon_0}(d_0 + x(t)) + V_{OC} \quad (1)$$

Equation one which represent the parallel plate model and there V_{OC} is the open-circuit voltage, S is the contact surface area d0 is initial displacement and ε_0 is the permittivity of the material. Even though this indicates the outputs, it is difficult to explain the outputs' polarisation in different scenarios and induction variations.

Dharamasena et al. developed the DDEF model overcoming such issued on parallel plate approximation.[18], [55].

$$E_Z = \frac{\sigma}{\pi\varepsilon} arctan\left(\frac{L/W}{2(Z/W)\sqrt{4(Z/W)^2+(L/W)^2+1}}\right) = \frac{\sigma}{\pi\varepsilon} f(z) \quad (2)$$

The DDEF equation, as given in equation two, contains a relationship between Width (W) and Length (L) of the TENG layer, surface charge density (σ), the permittivity of the material and the electric field (E_z) perpendicular to the centre of TENG layer. Here Z denotes the distance from the charged surface while undergoing a mechanical movement. Since this model developed based on electric field behaviour, it resolves problems associated with previous models.

DDEF model can predict different architectures' output behaviour, enabling more design capabilities over TENG with optimized electrical performance. For example, according to the model, when increasing the TENG surface area, it enhances the higher output, reducing the device's internal impedance. When internal impedance is higher, it can reduce the AC flow through the electrode, and the power output is comparatively meagre. Furthermore, when the TENG layer thickness decreased, that also favourably affect the enhancement of TENG. But the thickness needs to be sufficient to collect the required amount of surface charge for consistent power output generation. Typical textile architectures can be engineered to change the thickness and surface area without drastic affect on wearable performance. The TENG material's permittivity is another crucial parameter that governs the material's position at the triboelectric series. As previously mentioned, several textile polymers are positioned in the triboelectric series to select suitable material for optimized electrical output. Rather than using 2D fabric structures, the outcome can be enhanced using 3D fabric structures, enabling room for faster relative movements for triboelectric layers.

Additionally, to the surface and device optimization, sufficient contact separation or lateral movements with higher frequency and amplitude are also vital for higher output generation. The TENG devices need to be placed on the body, generating more energy due to increased mechanical movement (ex: underarm, knee, feet). Wearable properties need to be optimized either selecting suitable material or engineering the fabrication in a way that exhibits higher wearable performance. According to literature, knitted fabric-based structures have shown higher wearable characteristics compared with woven designs.

CHAPTER 3

3. RESEARCH METHODOLOGY

3.1 Introduction to The Chapter

This section is a detailed discussion of the research methodology to achieve the objectives of this research project. The focus of this project is to Systematically development of triboelectric nanogenerator with optimized wearable and electrical characteristics. In the first part of this project, a suitable triboelectric material was selected based on the layer's uniformity, voltage, current and charge outputs. The devices are systematically developed with triboelectric layers modification techniques such as printing, dip coating, and yarn coating to optimize the power generation and wearable characteristics. Selected wearable characteristics of the layer modification techniques are carefully analyzed with the sensitive textile testing equipment at the textile testing laboratory at the University of Moratuwa. Each identified methods' electrical performance is measured with precise equipment at Wolfson School of Mechanical, Electrical and Manufacturing Engineering at the University of Loughborough, United Kingdom. Finally, the best device was selected as the final prototype for the project.

3.2. Literature Survey

A comprehensive literature survey was carried out in General energy harvesting theory, material characterization using Scanning Electron Microscope (SEM), optical instrumentals, developing the TENG devices for wearable energy harvesting, printing, dip coating, yarn coating techniques along with high textile and wearable performance. To understand the behaviour of the TENGs, a background study was first performed since this is a modern technology to Sri Lanka, a thorough understanding required to produce world-class outputs.

3.3. Electrode Selection

TENG devices can be formed in fibre, yarn-based devices as well as fabric-based devices. This research project is focusing on developing a TENG device with excellent wearable and electrical performance. According to the literature, applying triboelectric material at the fibre-yarn stage and convert into textile fabric can lead to better wearable results. By considering that factor, the higher focus was given to yarn coating based TENG development. Under every concept, it is mandatory to select the best electrode material for better conductivity and induction effect. The electrode material was chosen to develop a fibre-yarn-based TENG device, silver-coated nylon yarn, and a staple spun stainless steel yarn (Table 3.1). The electrical resistance along the yarns' selected distance was measured to choose the best yarn with low linear resistance. According to the results electrode was fixed, and that was subjected to further developments.

Table 3.1:Characteristics of Core Yarn

Yarn	Yarn count	Type	Manufacturer
Silver-coated nylon	875 dTex	Continuous filament	Kitronik
Stainless steel polyester blended	787 dTex	Staple Spun	Credite

3.4. Selection of Triboelectric Material

According to the literature, it is mandatory to find two distinct materials in the triboelectric series to generate high charge density. Since this is a wearable development, it is evident that toxic or carcinogenic chemicals cannot be used. Furthermore, to achieve high wearable characteristics, the material should be compatible with textile engineering concepts while consistent with the electrode material. When looking into the past research activities, PDMS, PU, PTFE were highly used for TENG device manufacturing. Due to the difficulty of sourcing PTFE as a paster, Powder spray used for the development. Other materials and suppliers are given in Table 3.2.

Table 3.2:Chemicals for Triboelectric Layer Modification

Sample no	Type	Form	Manufacturing company
S1	Room temperature vulcanized rubber (RTV)	Paste	Dynatex
S2	PDMS	Paste	Dow Corning
S3	PTFE	Spray	Liqui molly
S4	Nylon 66 polyamide	Paste	New textile technologies

Once the triboelectric materials were identified, it was necessary to check the triboelectric behaviour of these materials. Therefore, initial testing for triboelectric behaviour was carried out with the bespoke testing procedures developed at the University of Loughborough.

3.5. Application of Material on Conductive Fabric

To check the material's triboelectric behaviour, a conductive fabric (Figure 3.1a) was knitted with the selected conductive yarn explained in section 3.1 and section 4.1. After preparing the fabric, S1, S2, S4 materials were applied as a paste on to the fabric using the screen-printing technique (Figure 3.1b). To have a comparison, it was necessary to apply the coating uniformly. Also, to get better results, the maximum coverage of the conductive layer was critical. A screen with the mesh count (number of mesh threads per inch) of 64 (SEM results show even coating with this mesh count) was selected.

S1 and S4 chemicals were directly applied to the fabric and cured at room temperature after 4 .5 hours as instructed by manufacturers. S2 was in two parts which was the resin and the curing agent. It was mixed according to the 10:1 resin to curing agent ratio and applied to the fabric, and then was kept in the oven for 6 minutes under $150C^0$for curing.

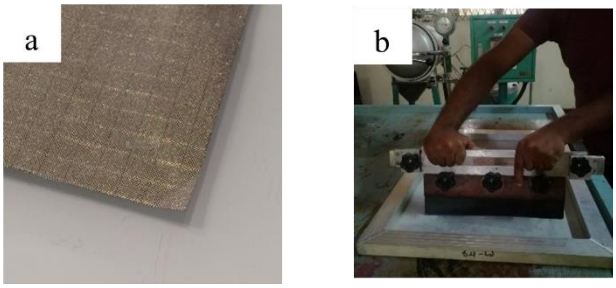

Figure 3.1: Triboelectric layer printing a) Conductive Fabric, b) Screen Printing Technique

The same number of printing cycles were applied using every paste to maintain uniformity over the thickness and material intake. SEM analysis was carried out to understand the micro-scale behaviour of the surface morphology.

3.6. Development of Yarn Coating System

After suitable yarn and triboelectric material were identified, the developments for core yarn were started. Firstly, the selected yarn was dip-coated with triboelectric material to get an even coating. After the experiment, there were many places without having a proper layer (Figure 3.2a, b) under this method. Also, there were air bubbles trapped inside the coating. Before applying the coating, triboelectric material was degassed inside a vacuum for one hour by considering those factors. The next experiment yarn was kept inside a plastic tube with a diameter of 4.5 mm and curing out inside the oven. The result (Figure 3.2c) was better than dip-coating, but since there is a requirement to coat a longer yarn, this was not an efficient and effective method.

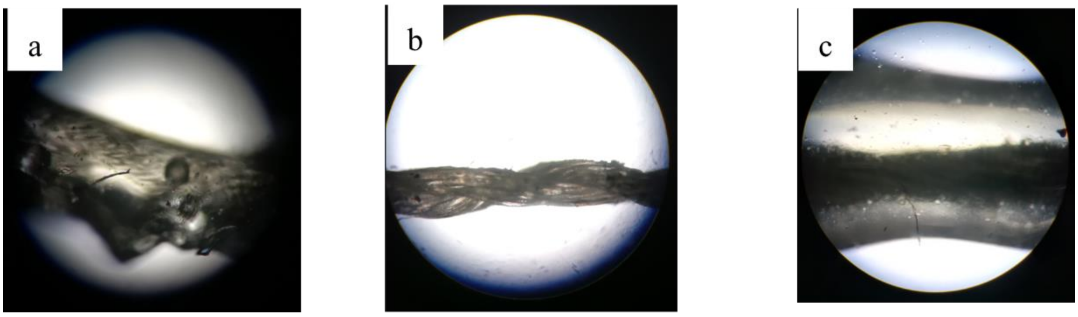

Figure 3.2: Optical Microscopic Image of Dip Coated Yarn a), b) at 50X, Microscopic Image of Yarn Coated with Tube c) at 50X.

Finally, an apparatus (Figure 3.3a, c) was developed to apply the triboelectric material into the yarn evenly based on the conical edged cylinder. The results were in the acceptable range, and new developments were carried out using this method. Triboelectric material was mixed with a respected ratio of resin to curing agent and kept inside a vacuum oven until the sample was degassed. After that, the material was filled into the coating chamber, and the yarn was pulled through the coating chamber. Yarn tension was controlled using a tension device at the value of 0.05 N. There was a mandatory requirement that yarn needed to be dried entirely before used for another process. To have evenness over the yarn, the drying required to be conducted without touching the yarn. After the yarn was released from the coating chamber, it was pulled through a laboratory-scale machine called mini stenter (Figure 3.3b). The stenter machine consists of a fabric movement system inside the chamber with a speed controller, four heating zones (Figure 3.3d), including the central heater and fan to generate stifling air.

The coated yarn was pulled out from the tip of the coating chamber (figure 3.3b) was dragged from the feeding side to the finishing edge of the stenter machine. There was a guide in the finishing edge that concentric with the coating chamber's tip, making the coated yarn straight based on the axis of the stenter machine. This method was helped to maintain uniform coating without touching the base of the stenter. Once the coated and dried yarn moves out from the guide at the finishing edge of the stenter machine, it was collected on to a rotating drum connected to the stenter machine rotating axis. The revolution per minute of the drum was controlled to keep the yarn 6 minutes inside the chamber. Since the speed and temperature (Figure 3.3e) can be controlled in the machine, the most suitable speed and temperature were selected after a few trials. Finally, yarn was running 6 minutes inside the heating zone at 150 ^{0}C temperature. The developed yarn was examined in SEM to check the evenness of the yarn. Multiple trials of the coating process were performed by altering the parameters to obtain an even yarn with the suitability for using in the next stages. Since single yarn electrical performance is insignificant to capture, the knitted fabric-based substrate was developed by considering the literature factors.

3.7. Development of Comparative Samples

The coated yarn was knitted in a flatbed knitting machine with gauge lengths of 3.5G (Figure 3.4b) (number of needles per inch in the device is 3.5) and 5G (number of needles per inch is 5).

Table 3.3: Dip Coated, Yarn Coated and Printed Sample Preparation.

Sample	**Method of preparation**	**Machine gauge**	**Thickness and area**
N1	Conductive yarn coated with a developed method and knitted	3.5G, 5G	8cm x 8cm 2.45mm thickness
N2	Fabric knitted with conductive yarn and dip-coated using triboelectric material	5G	8cm x 8cm 3.9mm thickness
N3	Fabric knitted with conductive yarn and printed using triboelectric material	5G	8cm x 8cm 3.4mm thickness

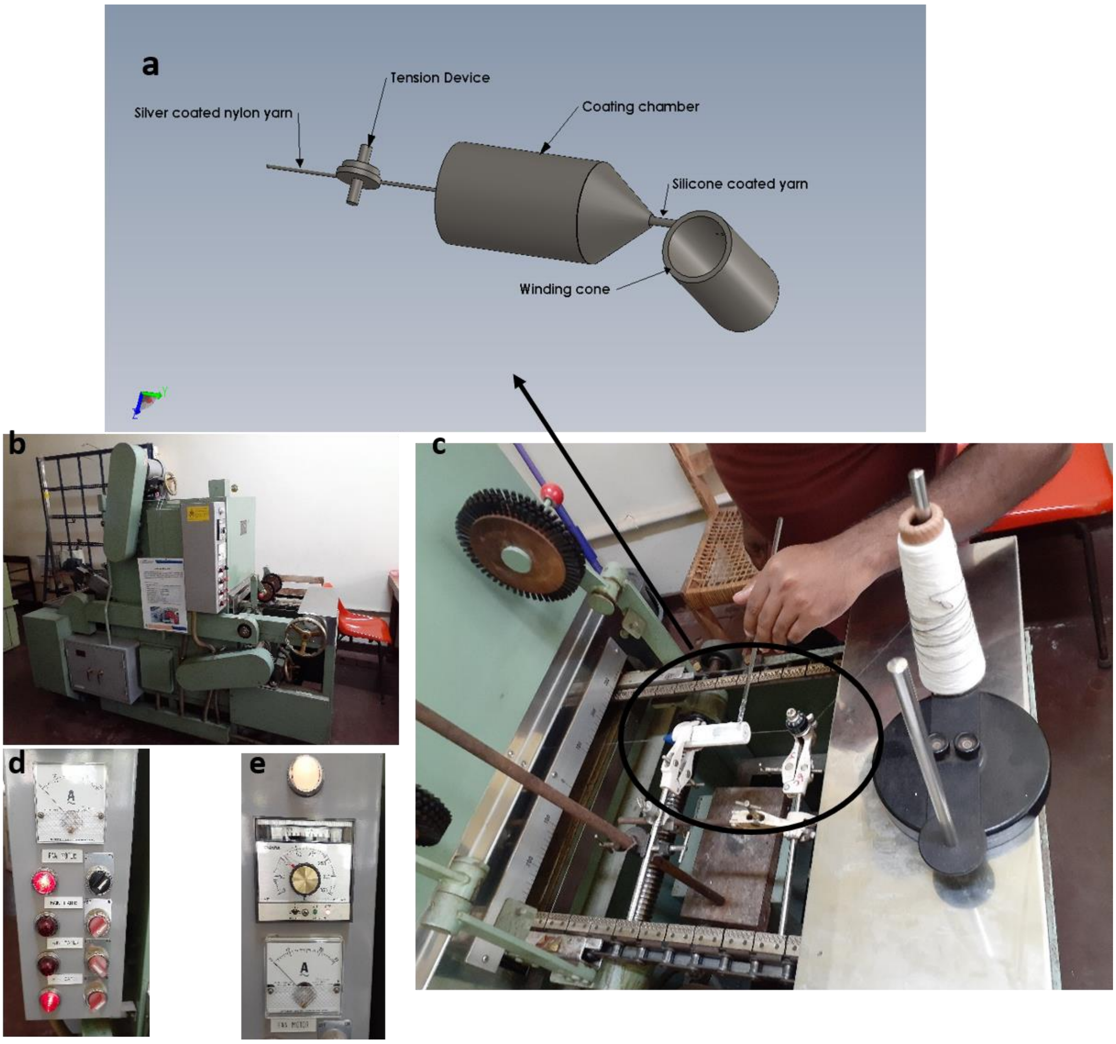

Figure 3.3:New Yarn coating method, a) Schematic Diagram for Bespoke Yarn Coating System, b) Mini Stenter Machine, c) Yarn Coating with the Developed System, d) Heater Controller of Stenter Device, e) Temperature Controller System

Due to the final yarn thickness, the 5G was the maximum possible machine for yarn coated samples. Besides yarn covered pieces, two samples were produced with printing and dip coating the triboelectric material over the electrode surface (Table 3.3). For the preparation of the printed (Figure 3.4c) and dip-coated (Figure 3.4d) sample, a piece of fabric was knitted with silver-coated nylon yarn in flatbed 5G knitting machines. A printed sample was prepared using the screen-printing device (Figure 3.4e) with fixed pressure(5N) and fixed speed (7 revolutions per minute). This ensured uniform printing over the sample.

After that the samples were tested for charge density, open-circuit voltage and close circuit current using the bespoke testing method with an electrometer-based system at the University of Loughborough UK.

Figure 3.4:Developed samples, a) Yarn Coated 3.5G Sample, b) Yarn Coated 5G Sample, c) Printed 5G Sample, d) Dip-coated 5G Sample, e) Printing Machine Used for Printed Sample Preparation.

3.8. SEM Examination for Surface Topography

SEM was carried out to investigate the surface topography and determine the extent of surface coverage by triboelectric material. Furthermore, Energy dispersive X-ray analysis (EDAX) and elemental mapping were conducted to determine the elemental composition on the surface to ascertain the availability of silver on the surface, which can cause troubles at TENG testing. Availability of silver on the surface indicates incomplete coverage of the coated triboelectric material. SEM examination was performed after preparation of dip-coated, printed, and yarn coated during the TENG manufacturing stage to get the information regarding the coating's surface thickness concerning fabric and diameter of the coating on the yarn because it is one of the governing factors for the generation of triboelectricity. Since conductive material used as the core of the yarn, complete coverage of the core is essential to prevent the leakage of charge to the 2nd electrode.

3.9. Testing for Charge Density, Voltage and Current

Dharmasena et al. have developed a unified theoretical model to elaborate on power generation over TENG [56]. They have created an experimental setup, as shown in Figure 3.5, to validate the theoretical model results. This test setup was used to measure the maximum open-circuit charge, maximum open-circuit voltage and maximum short circuit current of the samples in this research project.

Firstly, a set of tests carried out regarding the identification of suitable material. All samples were kept in an open environment for ten days to neutralize the charges already generated on the fabric. Later, all samples were checked against an Aluminium electrode (typically, material identification is carried out with conductive material) as the 2nd electrode (Figure 3.5(c)), and graphs were generated to compare the results.

This project aims to develop a textile-based TENG device; once the materials were identified, the secondary triboelectric material must be placed. Dharmasana et al. [2]. has previously used a PU bonded conductive fabric as a second electrode and triboelectric surface for their experiment, which has proven for excellent electrical performance. At first, a fabric was knitted with silver-coated nylon yarn. The secondary electrode was covered with a Bemis TP315 PU bonding layer with 102 microns, including a 51-micron adhesive part. When applying the recommended heat and pressure, the adhesive part melted and bonded between the fabric and the outer PU layer. After that, the prepared dip-coated, printed, and yarn coated samples were tested to determine each sample's electrical performance against the developed PU bonded sample. Finally, to analyze the Air Texturing technique's effectiveness, the secondary electrode replaced with an air textured yarn 5G knitted PU bonded sample. The best sample selected out of the previous analysis was used to develop the final prototype along with the developed air textured 5G knitted PU bonded sample.

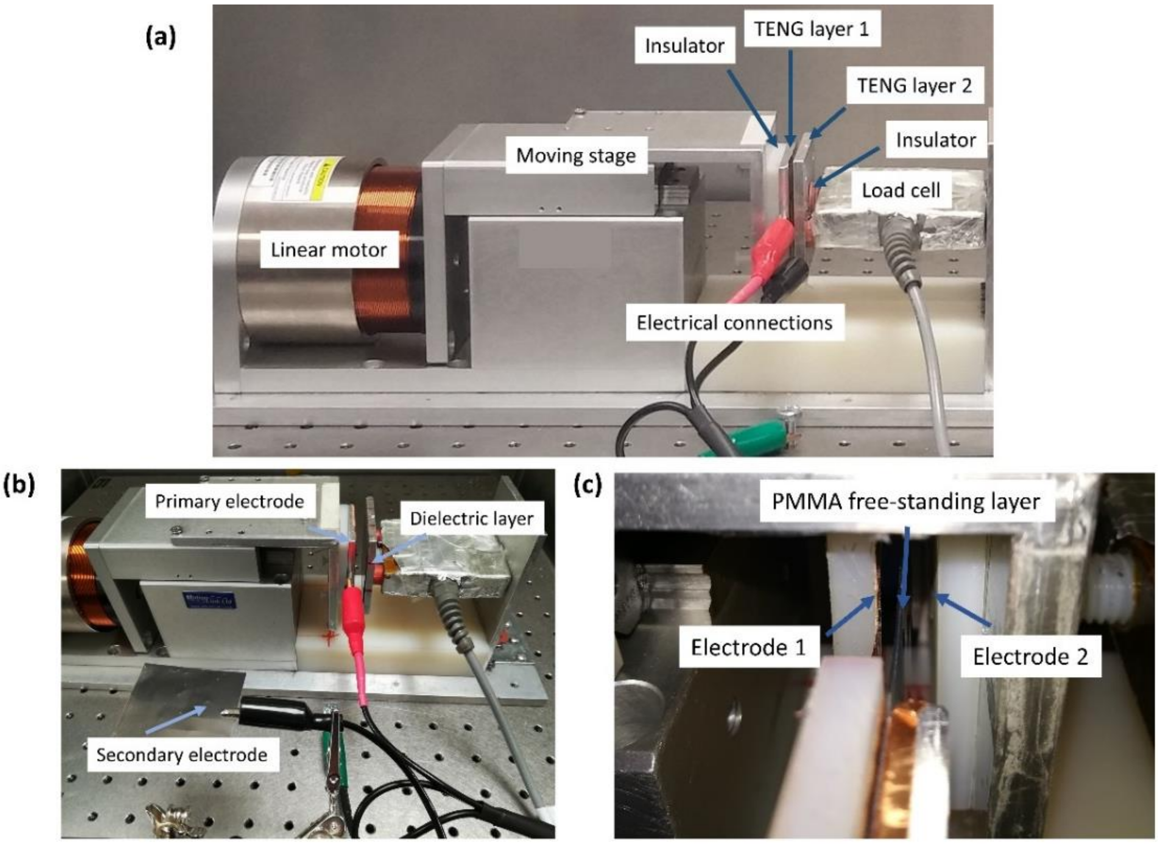

Figure 3.5: Electrical characterization setup, a) The Bespoke Test Setup for the Characterization of Vertical Charge Polarization TENGs. The Modification of the Design for the b) Non-parallel Secondary Electrode SETENG, c) Dielectric Free-standing Layer FSTENG.

3.10. Testing for Textile Performance

Since this project is more focused on wearable TENG development, it is essential to analyze given samples' textile behaviour. Most textile testing was conducted according to standards developed by the International standard organization (ISO), BS, ASTM, and AATCC. Air permeability testing, moisture management testing and stretch and recovery testing are selected from these testing methods. All these testing is carried out at 20 ± 2^{0}C temperature and 65 ± 4% relative humidity condition. Samples were kept inside the condition for 24h before conducting the test.

3.10.1. Air permeability testing

The SDL Atlas MO21A air permeability tester machine (Figure 3.6a) was used to conduct air permeability test. In this machine, there are clamping device to hold the fabric on a flat surface, six sets of test heads that can be used according to different test standards with the capability to prevent the air leakages from the edges of the test area, air pumping system and pressure gauge to measure the pressure drop from one side to another side. To investigate samples related to this project, the BS 5636 test method was used.

Table 3.4: Standards and specifications for air permeability test

Test Standard	Test Area	Test Pressure	Unit of Measure
ASTM D 3574	25 cm^2	125Pa	dm^3/s
EN ISO 9237	20cm^2	200/100Pa	dm^3/s
BS 5636	5cm^2	98Pa	$cm^3/ cm^2/s$

Each sample was kept inside the test head and waited till the machine got the pressure drop reading from one side to another. In this way, all models were supported, and the results are recorded.

3.10.2. Moisture management testing

SDL atlas moisture management tester (Figure 3.6b) machine was used as the measuring equipment for this test. By using this machine

- Absorption rate (moisture absorbing time of the fabric inner and outer surface)

- One-way transport capability (Liquid moisture one-way transfer from the fabric's inner surface to outer surface)
- Spreading/ Drying rate (Speed of liquid moisture spreading on the fabric's inner and outer surface) can be measured.

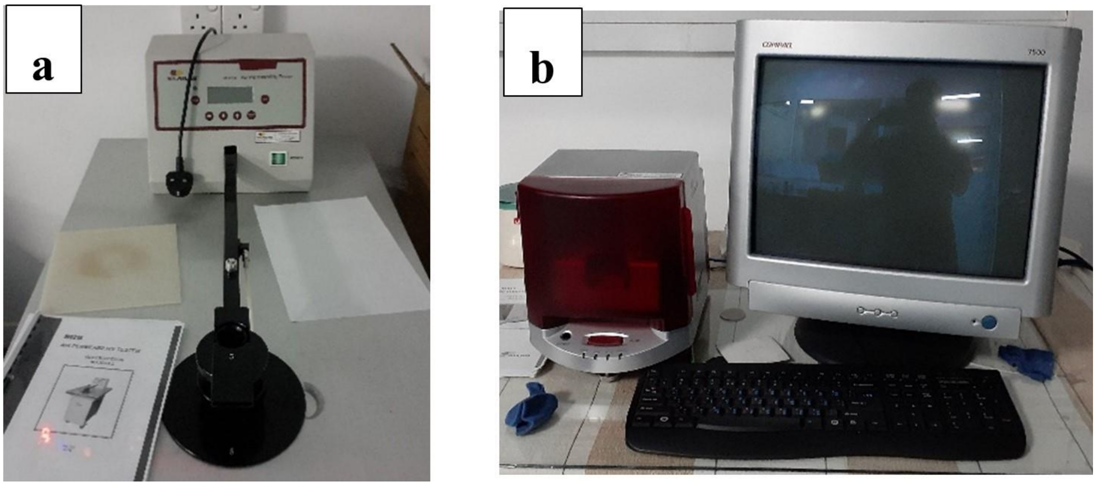

Figure 3.6: Wearable characterization machinery, a) Air Permeability Testing Machine, b) Moisture Management Tester

AATCC 195 standard was selected as the testing standard method for testing N1, N2, N3 and Air textured samples. The requirement to conditioning, specimens were prepared with 8cm x 8cm size, and it was kept inside the conditioned room for 24 hours. The moisture management tester contains two sensors on top and bottom to read moisture management properties. The specimen was kept between sensors and run the program accordingly. Once the program started, a top sensor pump releases few water droplets for 120 seconds to the fabric's top surface. All the above mention parameters were tested and calculated automatically, and the results were recorded.

3.10.3. Stretch and recovery testing.

For stretch and recovery testing, Instron tensile testing machine (Figure 3.7) was used. For standard testing, the method sample needs to be higher than the samples prepared. This testing was conducted with a custom testing method since the final result required a comparison of the modification methods. In Instron, the machine sample needs to be clamped into two jaws, and it will undergo stretch and recovery testing in standard atmospheric conditions. The stretch was generated by lifting the upper jaw again the fixed lower jaw. Samples are prepared in 4cm x 8cm dimensions.50.8mm (2 inches) has marked in the middle of the sample to clamp the pieces into machine jaws. Max load was selected as 34N. The machine was started, and once it was achieved the max load, the extension was recorded automatically by the software. After jaws were moved back to the return position, the sample was removed from the clamps. The recovery percentage was calculated by taking the displacement of the marked 50.8mm(2inches) in the sample. Several sets of trials carried out by increasing the max load.

Figure 3.7: Instron Tensile Testing Machine

3.11. Incorporate the Air Texturing Technique

To further optimize the power generation of the device, the secondary electrode was air textured. According to the literature, air texturing can lead to high linear density. At the same time, loops are formed [57] at different intervals over the electrode to instantly collect all the generated charges due to fibres' expansion. By looking at the DDEF model, the surface area has an impact on charge generation. Huyang et al. have found an increase in the charge density of knitted fabrics when the pores are closed[4] (Figure 3.8). Since there were limitations over knitting once the yarn is coated, instead of knitting with higher count, hypothesis was developed to increase the charge density by increasing the surface area of electrode with further opening of yarn using air texturing mechanism. Considering these factors before applying PU coating for the second electrode, Air texturing was carried out at the yarn processing laboratory at the University of Moratuwa.

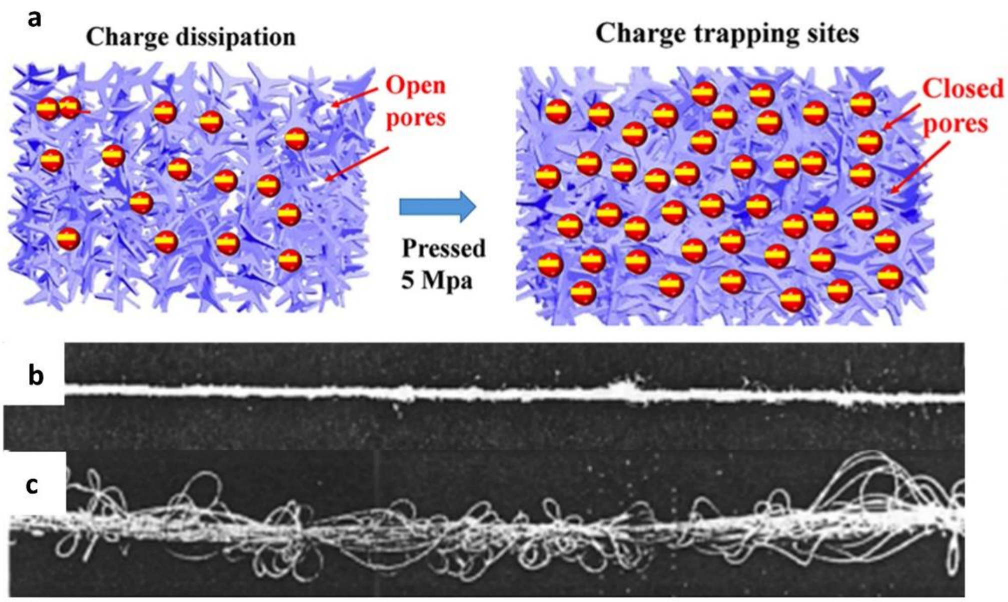

Figure 3.8: Incorporation of air texturing mechanism, a) Charge Trapping Increased When Closing the Pores, b) Before Air Texturing, b) After Air Texturing Yarn Reprinted from Ref [4], [57]

Source : [4], [57]

Machine parameters are given in Table 3.5. The silver-coated nylon yarn was air textured using this formula and consequently knitted using gauge five machines at the knitting laboratory.

Table 3.5: Air Texturing Parameters

Parameter	Value
Overfeed	10%
Draft	1.4
Temperature	100 C^0± $2C^0$
speed	60 m/ min

Two samples were prepared with the air texturing technique and without the air texturing technique. After knitting sample was bonded with PU bonding material which used for previous analysis using a pressure pad. This was used as the secondary triboelectric surface, where the last recognised best sample used as the primary. Those samples were subjected to contact and separation as previous to analyse the enhancement of the outputs.

CHAPTER 4

4. RESULTS AND DISCUSSION

4.1. Selection of Yarn

The yarn selection is one of the most crucial stages in this research project since conductivity is a significant factor in TENG's output[1]. The yarn selection was made based on the linear resistance. Linear electrical resistance was measured by keeping the yarns on the table with equal tension. The resistance was measured by placing the multi-meter probes in the given distance (Table 4.1).

Table 4.1: Linear Resistance of Selected Yarns

Type	Resistance at 1cm (Ω)	Resistance at 5cm (Ω)	Resistance at 10cm (Ω)
Silver coated nylon	1.5	3.2	5.1
Staple spun stainless steel polyester	328	853	1920

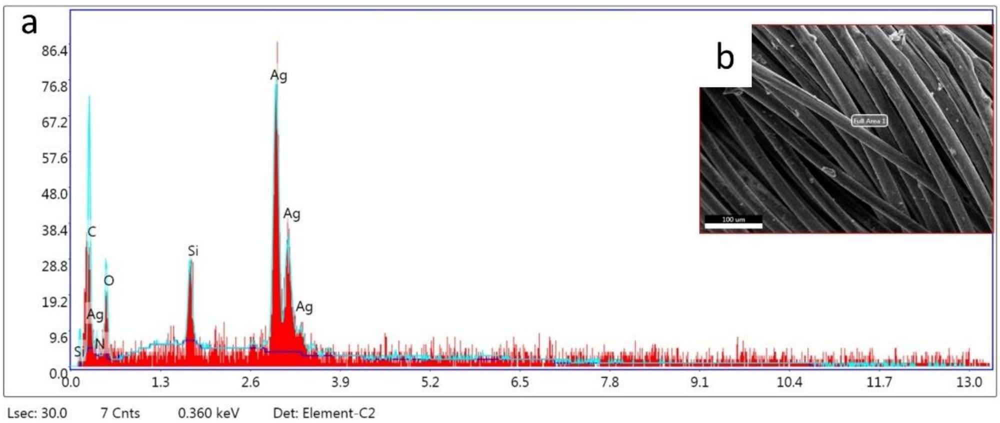

eZAF Smart Quant Results

Element	Weight %	Atomic %	Net Int.	Error %	Kratio	Z	A	F
C K	18.94	41.65	9.13	14.78	0.1165	1.2156	0.5063	1.0000
N K	3.22	6.07	0.61	92.10	0.0065	1.1914	0.1697	1.0000
O K	21.05	34.75	4.35	24.88	0.0309	1.1699	0.1256	1.0000
SiK	5.21	4.90	6.66	20.14	0.0375	1.0761	0.6605	1.0127
AgL	51.59	12.63	27.47	10.49	0.4458	0.8121	1.0643	0.9998

Figure 4.1: EDAX Report for a) Silver Coated Yarn, b) sample area

Staple spun fibres based yarns contain short staples, which can lead to disruption for the conductivity. But the silver-coated nylon yarns are much more versatile, with silver coating throughout the yarn giving a better conductivity than the staple spun yarns. The EDAX report generated for the yarn confirms that 51.59% weight percentage silver is available on the surface with giving better conductivity (Figure 4.1).

Based on the results, silver-coated nylon yarn selected as the core yarn and the base for every other sample.

4.2. Selection of Triboelectric Material

4.2.1. SEM result comparison

After samples were coated evenly using the screen-printing method on to conductive fabric surface, samples were prepared with the dimension of 10*10 cm. Since the fabric was already conductive, testing on the SEM was carried out without using the conductive coating on top of the sample.

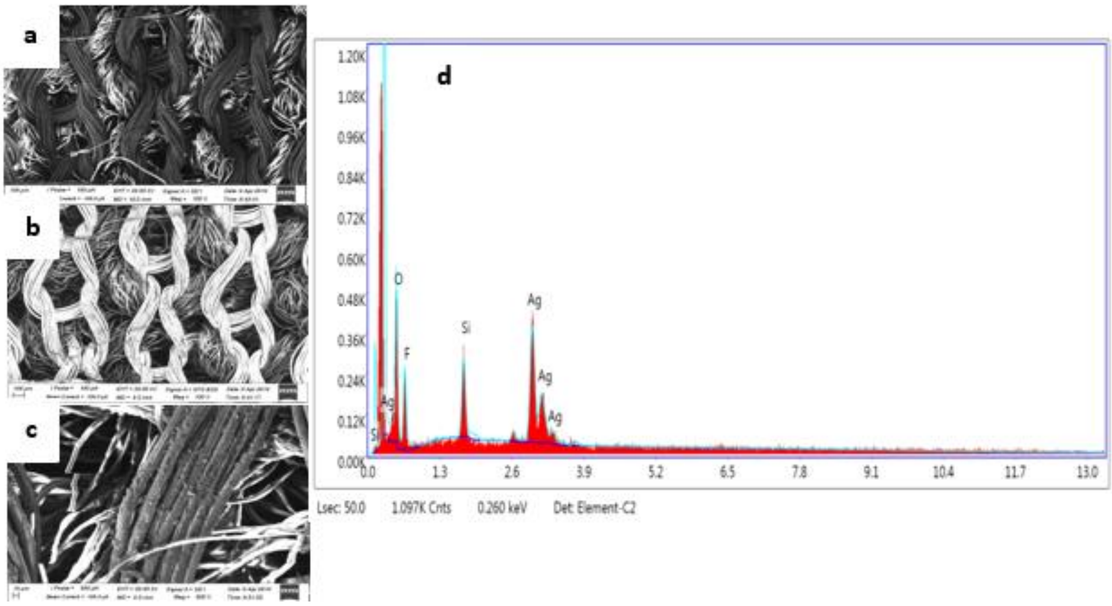

Figure 4.2: SEM of a) RTV Silicone Coated Sample 100X. b) Back Scattered Image 100X. (c) 500X. EDAX Report of d) RTV Silicone

EDAX report was generated to get an understanding of materials on the surface. According to results, RTV silicone (Figure 4.2), PTFE (Figure 4.4), and polyamide (Figure 4.3) samples consisted of silver residues on top of surfaces.

The main reason for that was that the material was scattered after curing. Because of the requirement of even coating, without doing further changes to any samples, that were proceed to the next stage. When considering the silicone sample (Figure 4.5), it consisted of better coverage on given conditions. To get more clarity to select the suitable material, charge density, open-circuit voltage and close circuit current measured at the next stage.

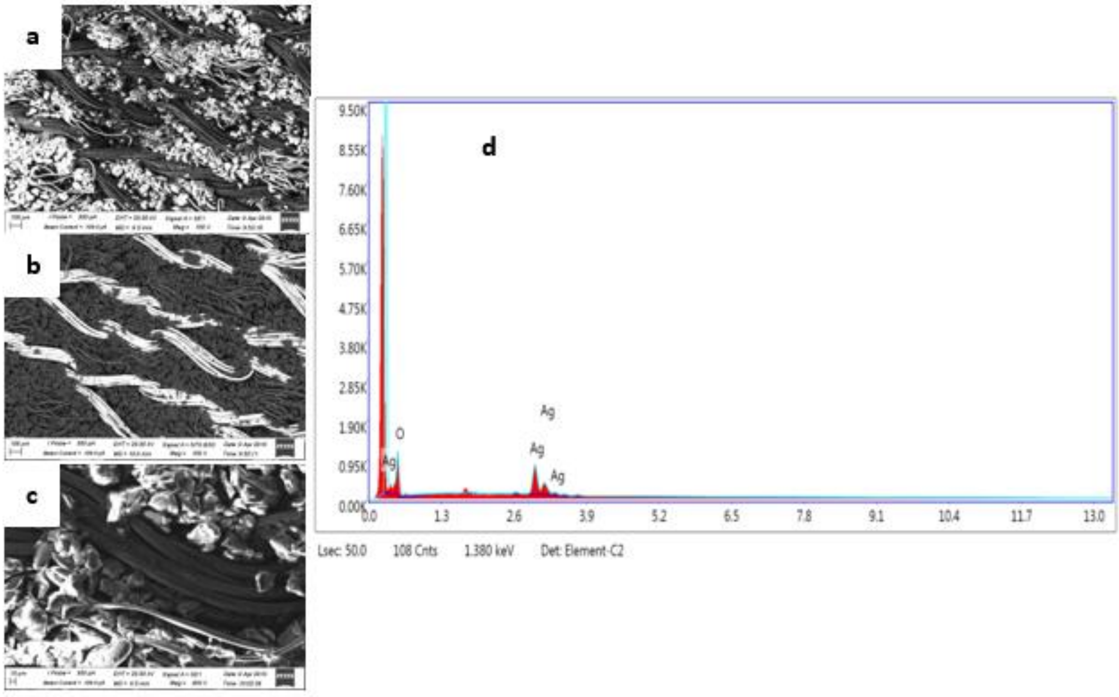

Figure 4.3: SEM of a) Polyamide Coated Sample 100X., b) Back Scattered Image 100X., c) 500X., d) EDAX Report of Polyamide

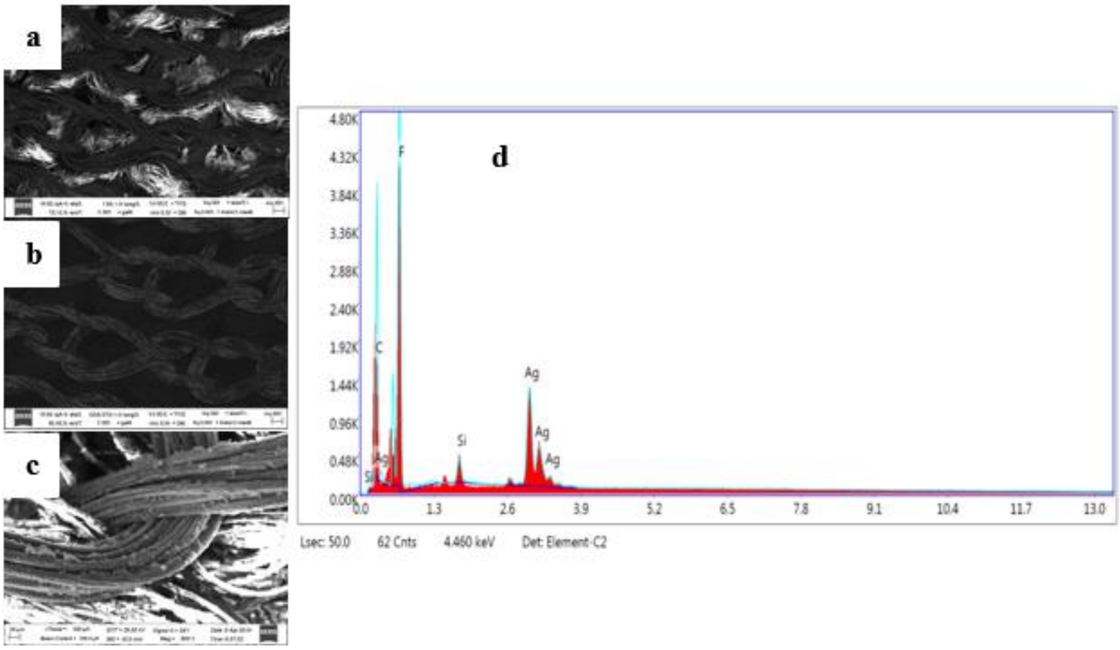

Figure 4.4: SEM of a) PTFE Coated Sample 100X., b) Back Scattered 100X., c) 500X., d) EDAX Report of PTFE

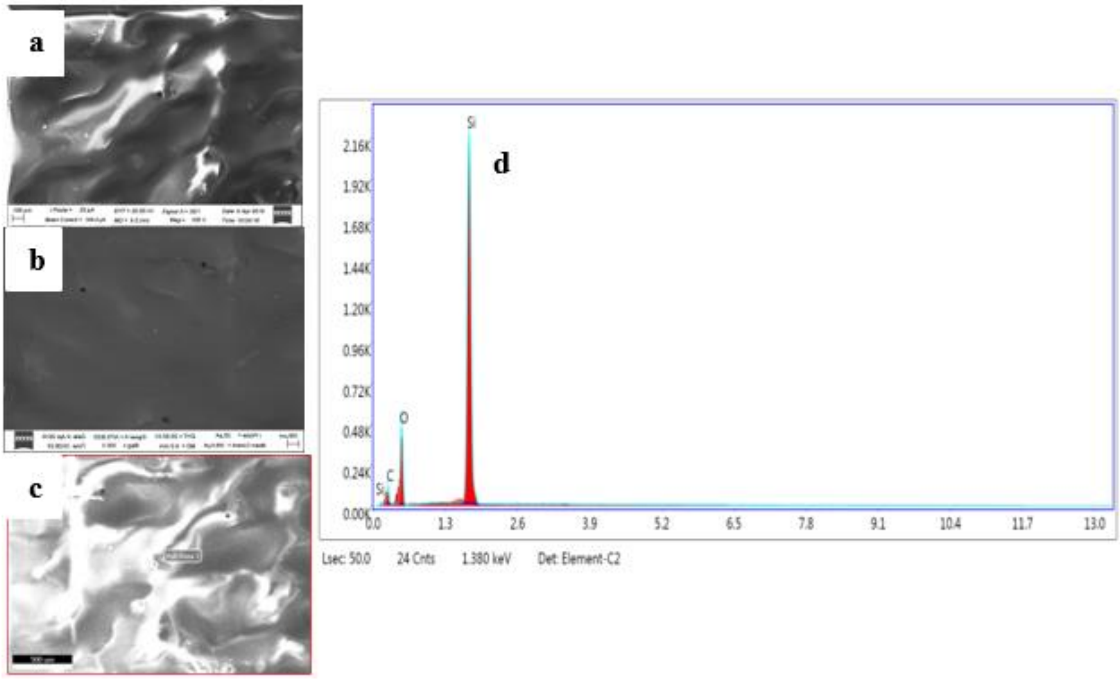

Figure 4.5: SEM of a) Silicone-coated Sample 100X., b) Back Scattered Silicone 100X., c) 500X. d) EDAX Report of Silicone

4.2.2. Comparison of Charge, Voltage and Current

All samples were subjected to contact separation TENG testing with the Al layer, as shown in Figure 4.6, which acts as a triboelectric layer and electrode.

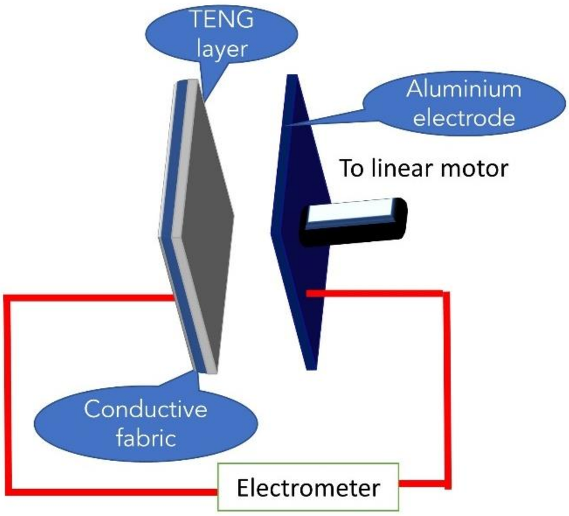

Figure 4.6: Schematic of Electrical Result Characterization of the Triboelectric Layer Selection Process

Maintaining uniform temperature and humidity factors are very important since TENG behaviour can drastically change with these conditions [2]. Thus, the temperature was kept at 19.6 C^0 while relative humidity of 58.2 maintained during the testing. All samples were prepared 5 cm * 5 cm for electrical characterizations. The selected motion profile is 1 mm displacement at 2 Hz frequency. The motion profile is validated using the load cell readings (Figure 4.7) mounted to the stationary part of the bespoke device. According to the graphs in bellow figures (Figure 4.8, Figure 4.9, Figure 4.10), results can be summarized (Table 4.2).

Table 4.2:Comparison of Charge, Voltage and Current of Different Materials

Sample	**Max charge (nC)**	**Maximum Open circuit Voltage (V)**	**Maximum Close circuit current (nA)**
PTFE	0.595	1.3873	18.4
RTV	1.105	2.6	137.98
Silicone elastomer	8.173	30	158.71

According to test results summarized in Table 4.2, Silicone elastomer has given better results in all three aspects. TENG typically generates asymmetric current output due to the nature of contact used for the current generation. It is evident that the most accurate result can be obtained by the half-cycle, which is responsible for the separation rather than the contact position[58]. By considering these factors when recording the maximum current value, the maximum of the positive peaks (start half-cycle was selected as the separation position and that was responded to positive side) was chosen in every graph (Figure 4.8).

When considering the triboelectric series, the Silicone elastomer is more negative compared with Al. Furthermore, the PTFE lies in between silicone elastomer and Al which is comparatively less negative than silicone elastomer. This could result in lower output for PTFE compared with the silicone elastomer. Moreover, the scattering of the materials during the testing process due to the soft binding of molecules, as shown in SEM, can lower the PTFE value. Even though RTV silicone contains silicone due to the other cross-linking materials used within it can cause low result generation. Unfortunately, it is hard to find substantial theoretical evidence for resulting low power from RTV silicone materials. By considering the open-circuit voltage, close-circuit current, charge density and surface coverage with better evenness, the Silicone elastomer selected as the primary triboelectric material for further developments.

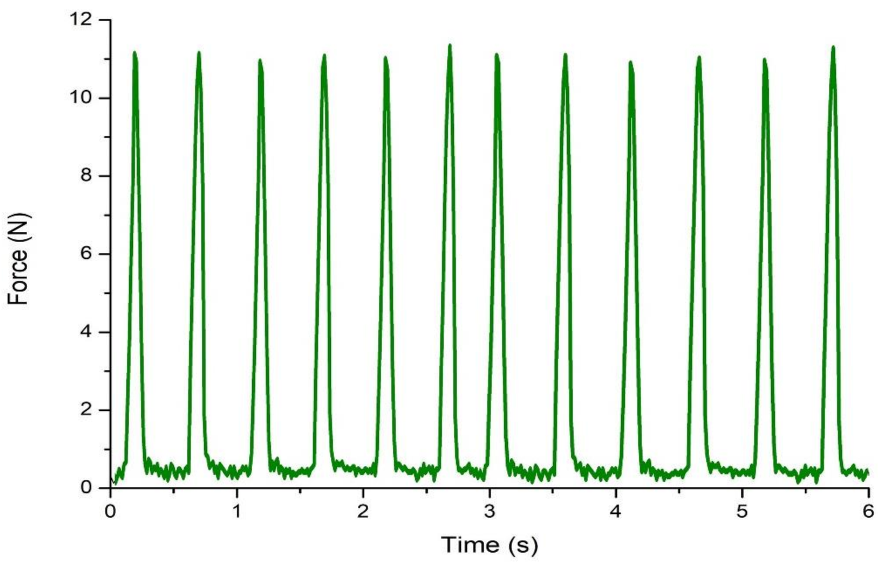

Figure 4.7: Motion Profile Used for Characterization

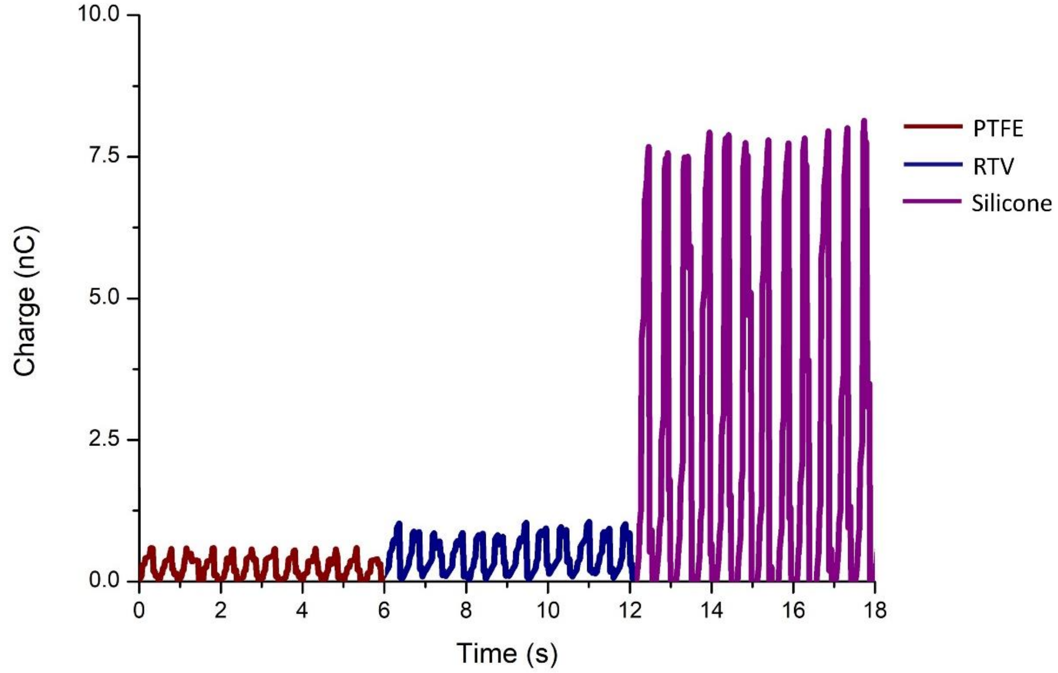

Figure 4.8:Comparison of Max Charge Generation for Selected Triboelectric Materials

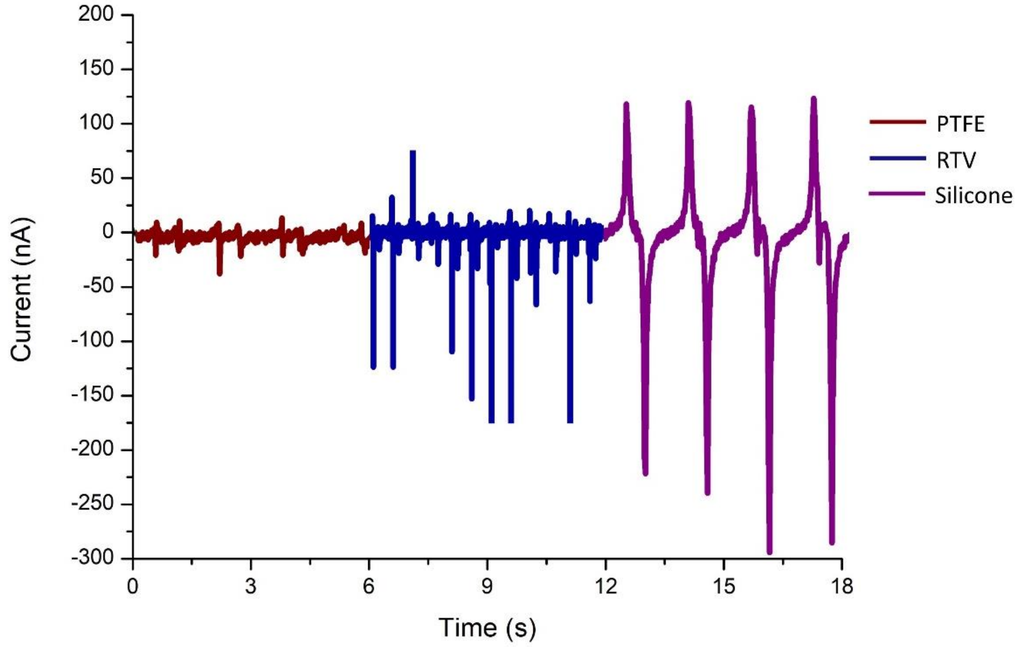

Figure 4.9:Comparison of Close Circuit Current for Selected Triboelectric Materials

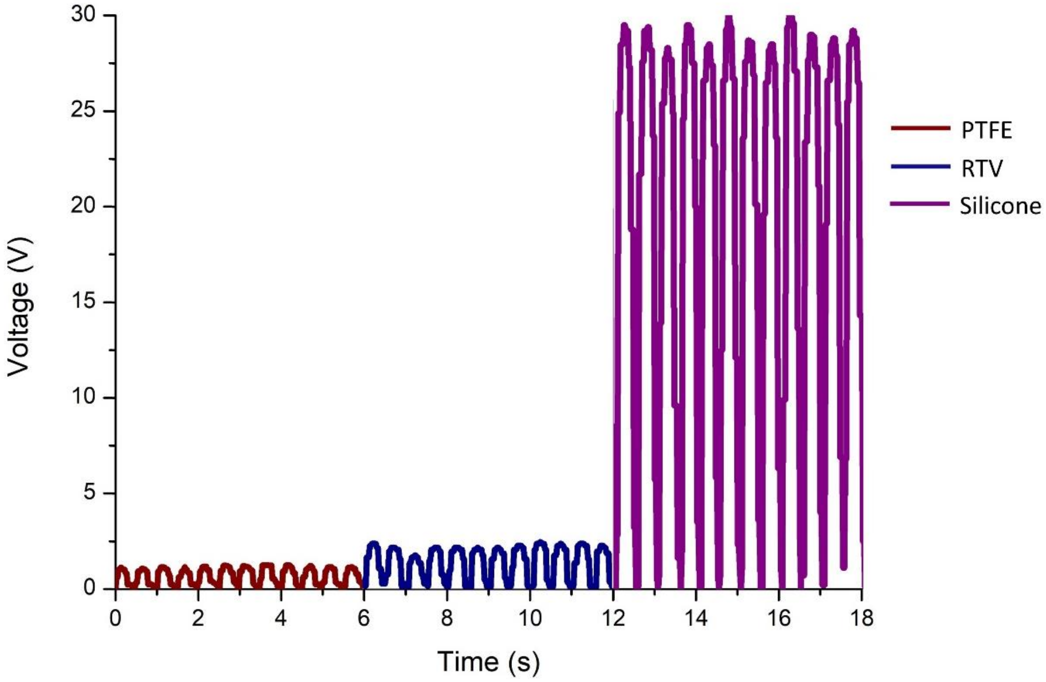

Figure 4.10:Comparison of Open Circuit Voltage for selected Triboelectric materials

4.3. Selection of Triboelectric Layer Application Technique

4.3.1. Comparison of the morphology of printed, dip-coated and yarn coated samples.

After dip-coated, printed, yarn coated samples were prepared, SEM observation was carried out to analyze each category's surface morphology.

All three samples were shown to have better coverage, and there was no presence of conductive silver material outside. EDAX report and elemental mapping confirm the complete coverage of Silicone over the surfaces. When considering the dip-coated sample (Figure 4.11), the SEM image conforms to the silicone coating uniformness with1.3491 mm thickness for one side of the fabric.

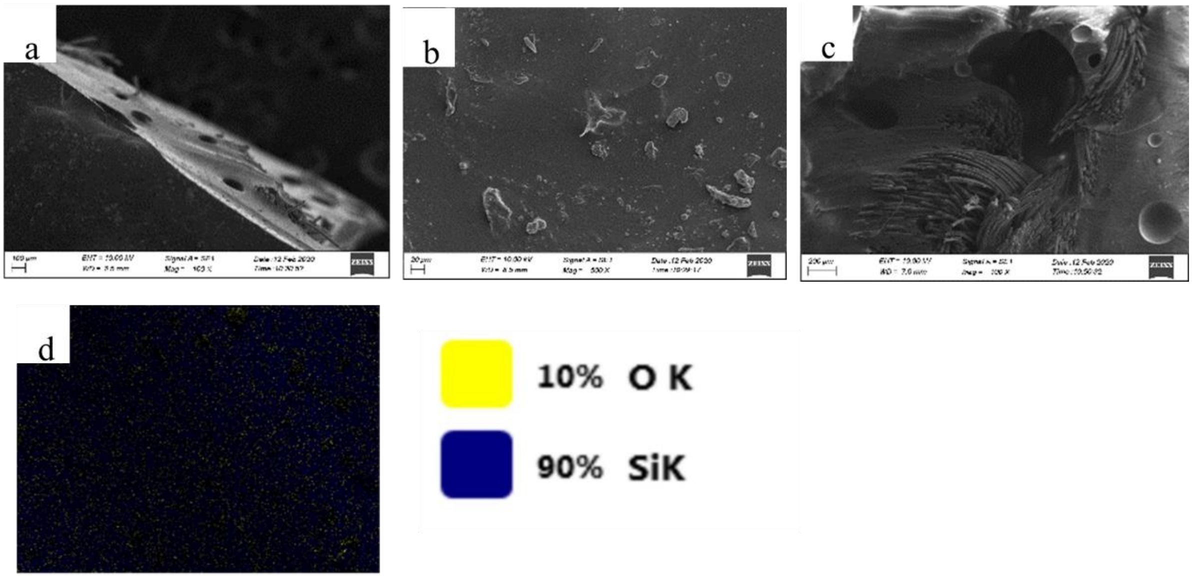

Figure 4.11: SEM images of Dip-coated Sample a) Side View of the Sample 100X, b) Surface of the Sample 50X, c) Cross-section of the Sample 200X, d) Elemental Mapping of the Top Surface of the Sample.

Because of the printing with a mesh, there was a possibility to have very few holes (small unprinted areas due to mesh structure) in the printed sample (Figure 4.12). SEM images have confirmed that the printed sample surface was uniformly coated with 1.279 mm surface coating with a few small unprinted areas (Figure 4.12 (c)). Since Silicone's peak in the EDAX report, the surface coverage can be considered non-conductive.

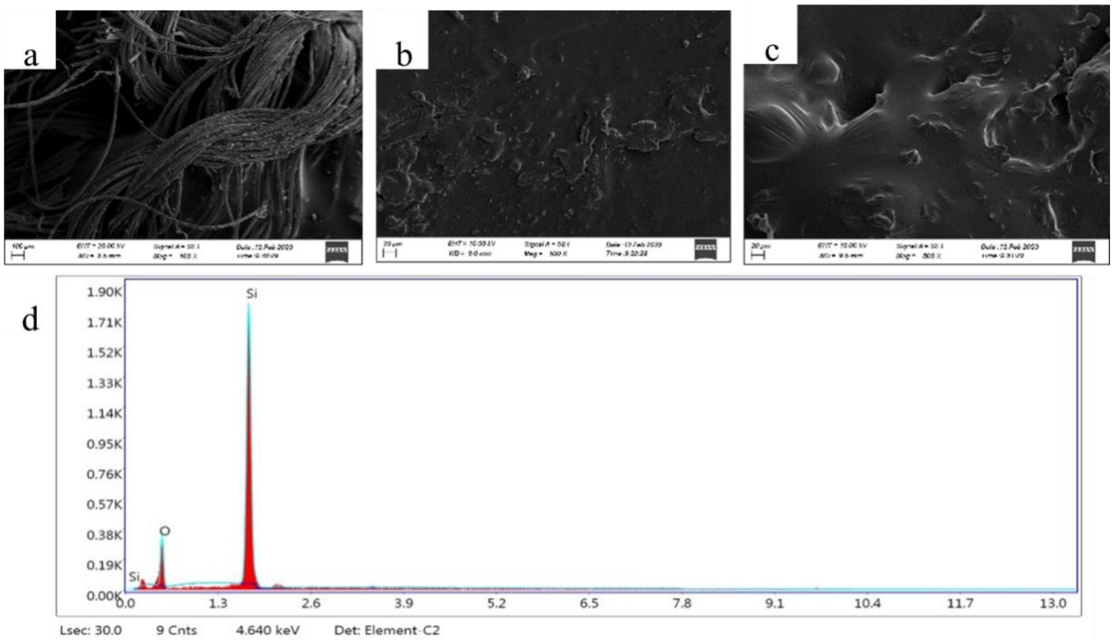

Figure 4.12:SEM images of Printed Sample a) Unprinted Side of the Fabric Sample 100X, b) The Printed Surface of the Sample 50X, c) Unprinted Areas in the Surface of the Sample, d) EDAX Report for the Surface.

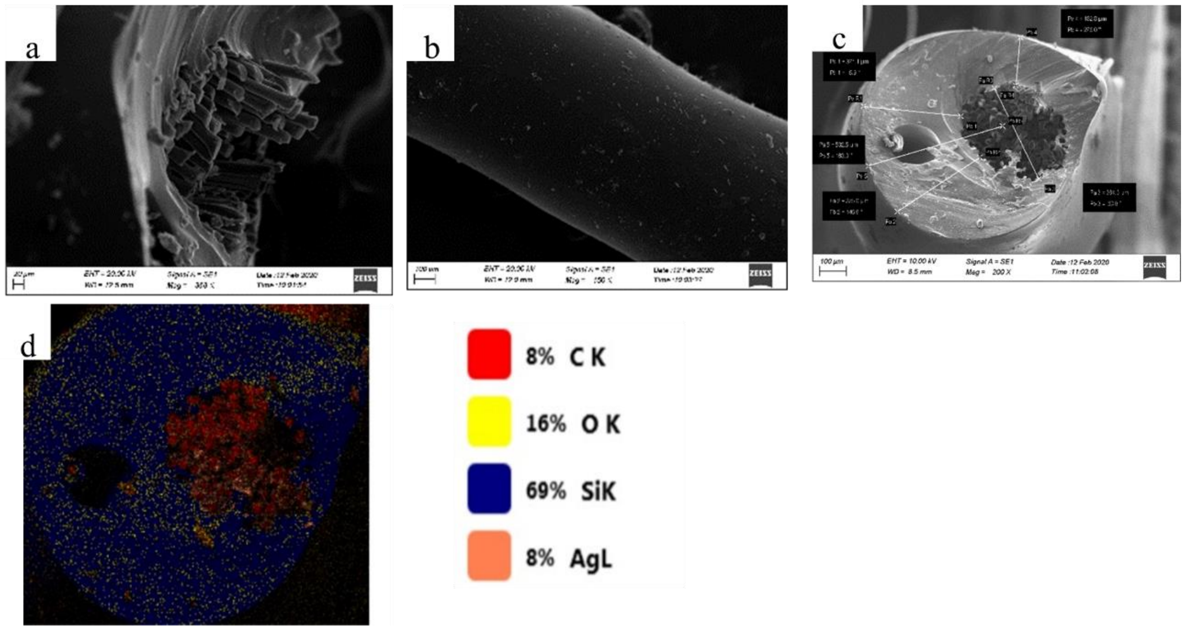

Figure 4.13: SEM Images of Yarn Coated Sample a) Side View of the Yarn 368X, b) Surface of the Coated Yarn 150X, c) Cross-section of the Yarn 200X (d) Elemental Mapping of Coated Yarn.

Yarn coating has been the critical area of this project, and thus the coated samples were carefully examined (Figure 4.13). SEM images confirm that the yarn was covered with a silicone coating of an average of 309.6 µm (Figure 4.13c) after several coating trials. It was challenging to cut the surface of the yarn perpendicularly. Figure 4.13b is confirmed that the surface smoothness is achieved with the developed yarn coating system. When considering the EDAX report (Figure 4.14) for coated yarn, the coating has completely covered the conductive surface, which satisfies the requirement to manufacture TENG.

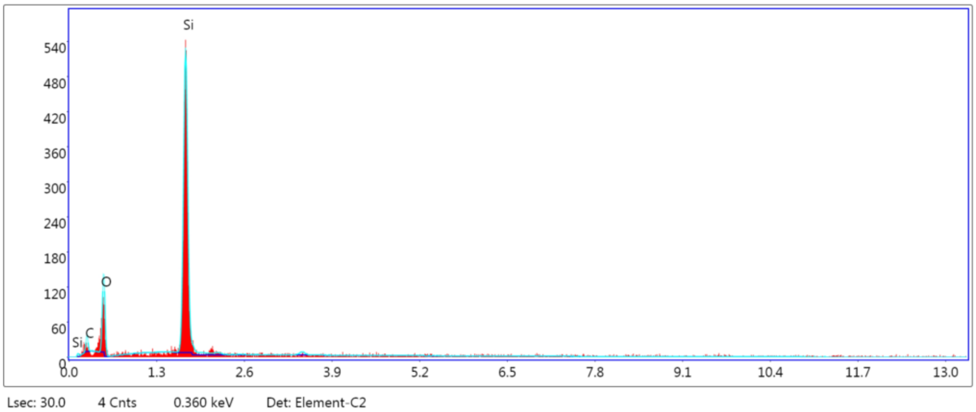

eZAF Smart Quant Results

Element	Weight %	Atomic %	Net Int.	Error %	Kratio	Z	A	F
C K	19.90	30.62	4.13	24.80	0.0265	1.0769	0.1239	1.0000
O K	33.54	38.74	23.25	14.13	0.0828	1.0311	0.2394	1.0000
SiK	46.56	30.63	138.36	4.12	0.3879	0.9380	0.8879	1.0006

Figure 4.14: EDAX report for Silicone Coated Yarn.

4.3.2. Comparison of charge, voltage and current for structure modification

After finalizing core yarn as the silver-coated nylon and triboelectric material as Silicone, the structural modification-related testing was carried out. According to the description given in section 3.5 and section 3.6, four samples were tested. Testing was carried out with the same mechanism as before at the University of Loughborough. All models were subjected to contact separation TENG testing with a polyurethane-coated fabric layer of the sample size of 5 cm* 5 cm (Figure 4.15). The selected motion profile is 1 mm displacement at 1 Hz frequency. According to the graphs below (Figure 4.16, Figure 4.17, Figure 4.18), results can be summarized (Table 4.3).

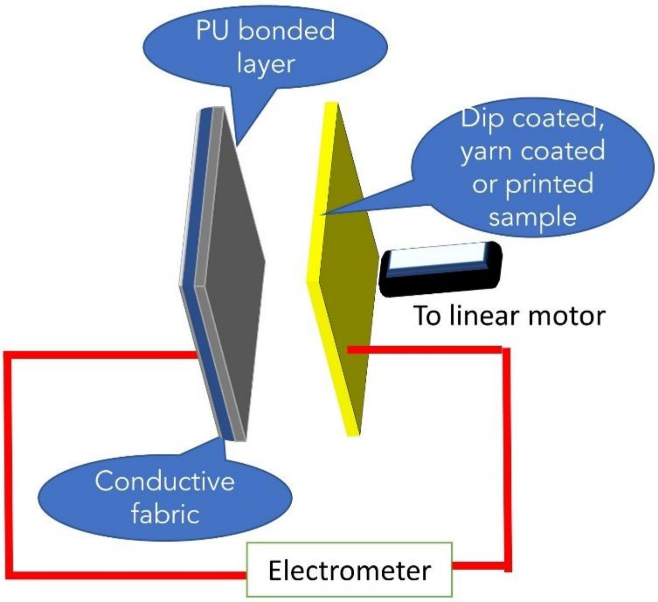

Figure 4.15 : Schematic for Electrical Characterization of Triboelectric Layer Application Process Analysis

Table 4.3: Summarization of Charge, Voltage and Current for Different Application Methods of the TENG Layer

Sample	Max Current (nA)	Max Voltage (V)	Max Charge(nC)
Dip Coated 5G	10.99	4.92	1.973
Printed 5G	43.19	17.33	4.797
Yarn coated 5G	60.10	34.53	11.45

When comparing the thickness of the triboelectric layers, the dip-coated sample had 1.3491 mm while the printed sample had a 1.279 mm thickness. Furthermore, the SEM analysis of the dip-coated sample showed uneven coating through the fabric surface. The yarn coated sample thickness was 309.6 µm, which is comparatively very low with the other two methods. According to Dharamasana et al. [56] increase in thickness leads to the reduction of charge density, thus reduce current and voltage.

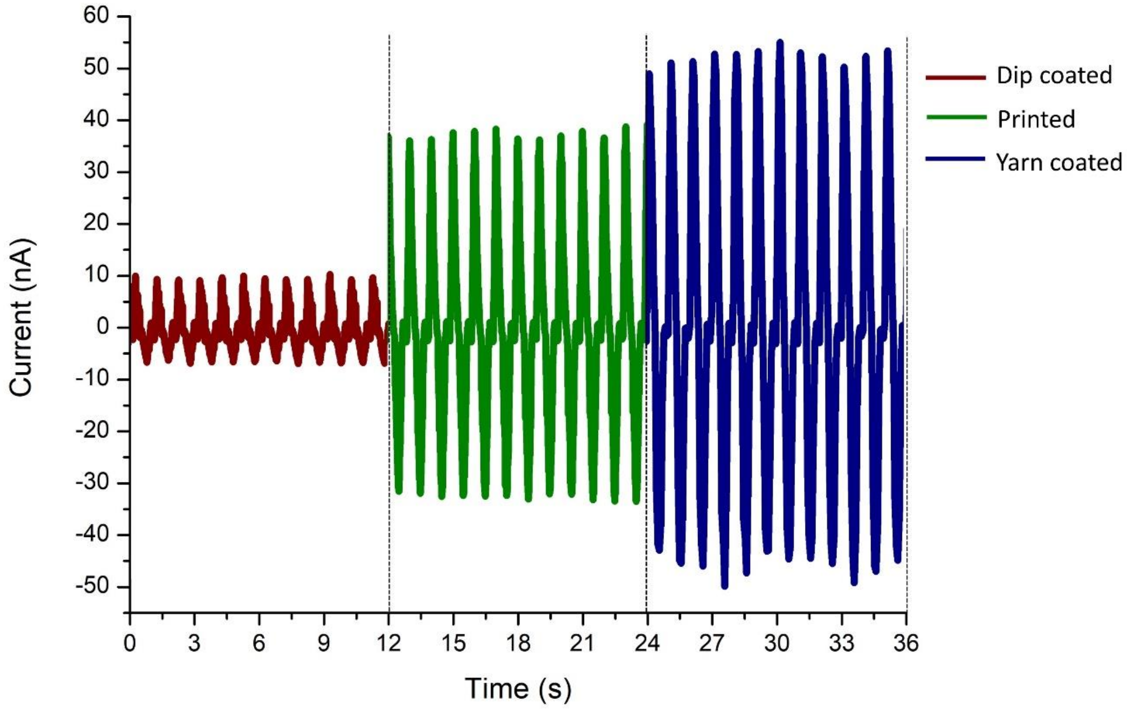

Figure 4.16: Current Comparison for Different Layer Modification Techniques

Moreover, the surface area is one of the critical factors in determining the triboelectric nanogenerators' output. The knitted structure can create an increase in power outputs, as described in chapter 2. The dip-coating and printing didn’t emphasize that feature as the yarn coating method. Additionally, in the yarn coating method, the triboelectric layer was coated around the electrode with low thickness, facilitating more induction to the electrode surface. The surface roughness of the yarn coated sample also acts as a favourable factor for better contact and separation. These factors affect the increase of the charge density and voltage and current increased accordingly.

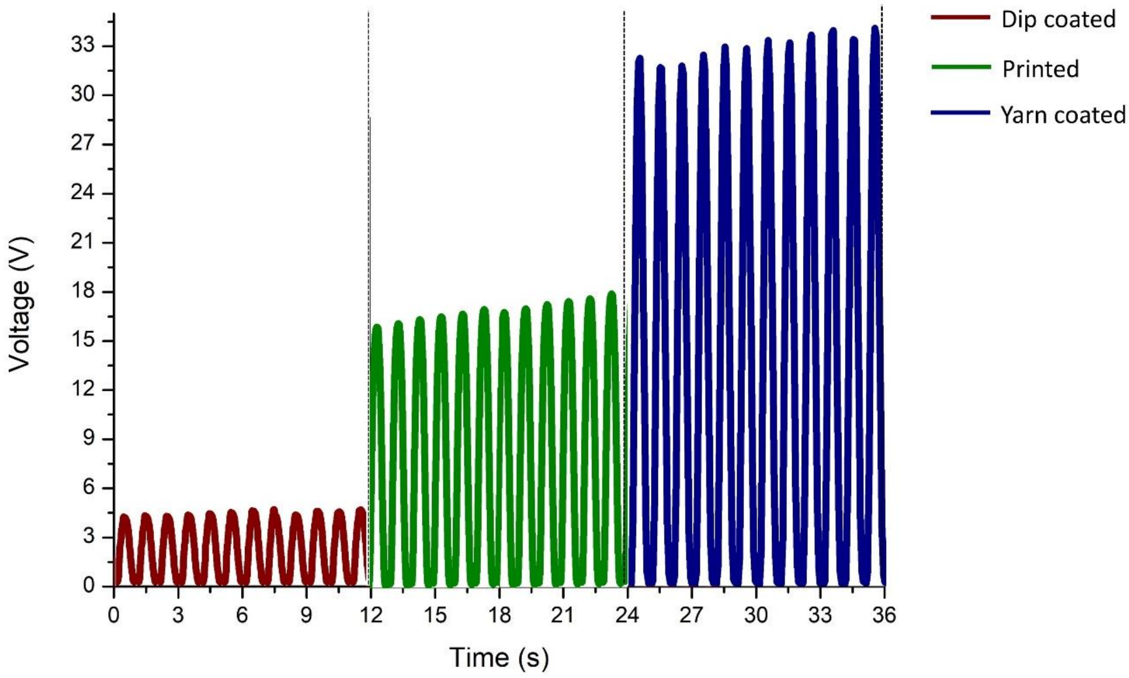

Figure 4.17: Voltage Comparison for Different Layer Modification Techniques

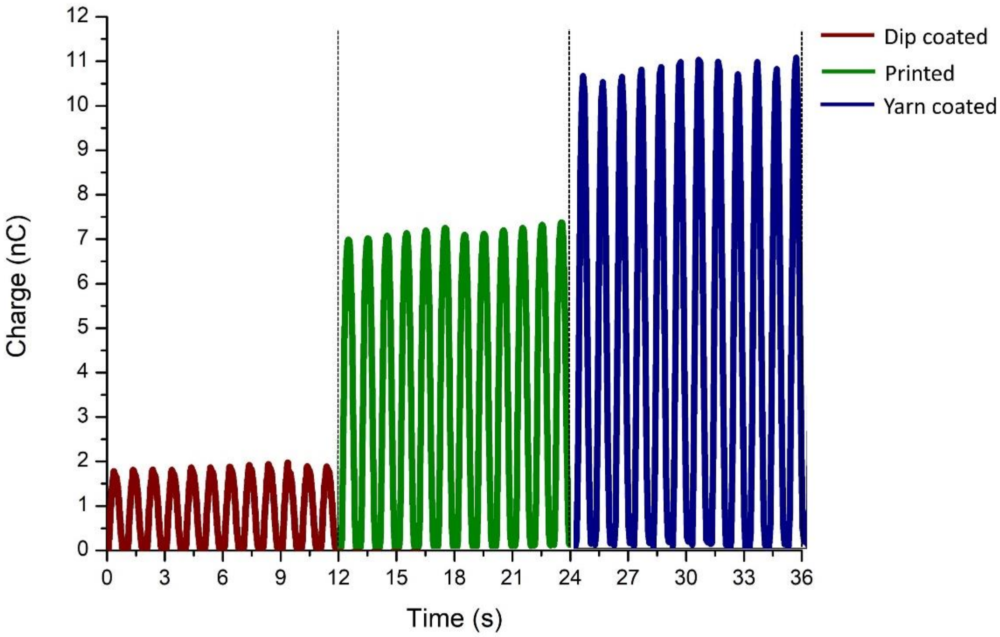

Figure 4.18: Charge Comparison for Different Layer Modification Techniques

By observing the results and the factors mentioned above, the highest output for Short circuit current of 60.10 nA, the open-circuit voltage of 34.53 V, and open circuit charge density of 4.58 μC/m^{2}received for the yarn coated 5G sample.

When comparing results related to the gauge factor (Figure 4.19), there is an increase in the results with the increase of the gauge. That is due to the increase of induction of charges due to the increase of the electrode's surface area under the triboelectric surface.

To validate this observation, the secondary electrode is air textured, expecting an increase in results.

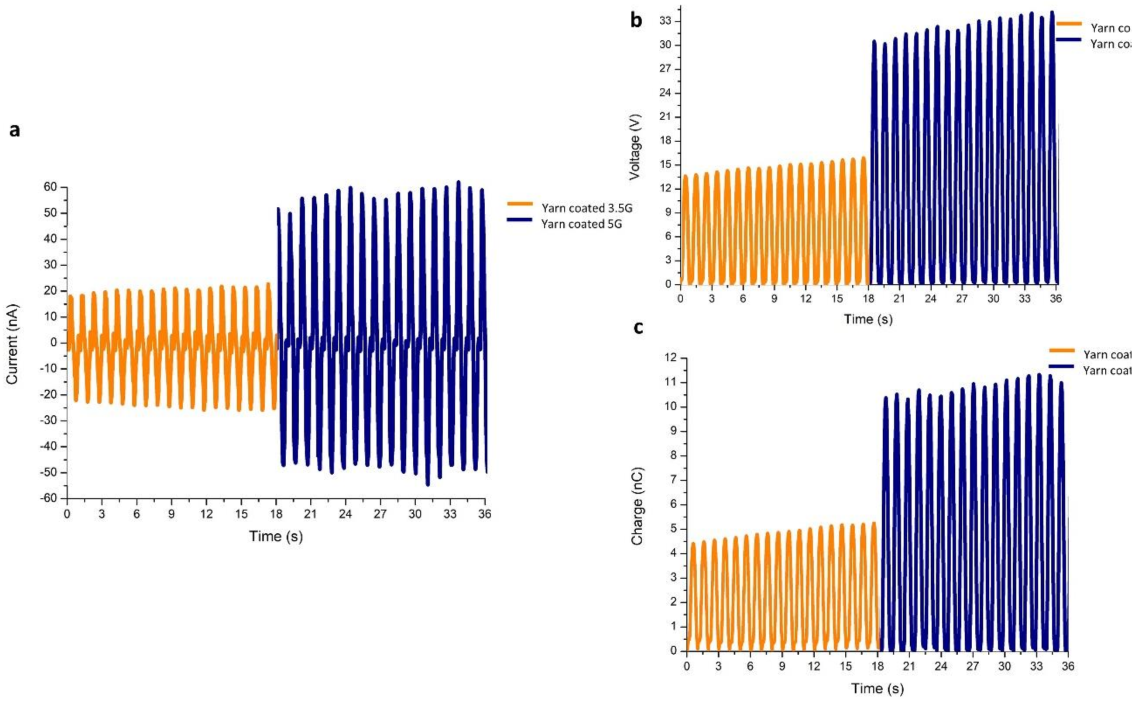

Figure 4.19: Electrical Output Comparison Between Yarn Coated 5G and 3.5G Samples a) Short Circuit Current, b) Open Circuit Voltage and c) Open Circuit Charge

4.3.3. Final prototype with air textured secondary electrode

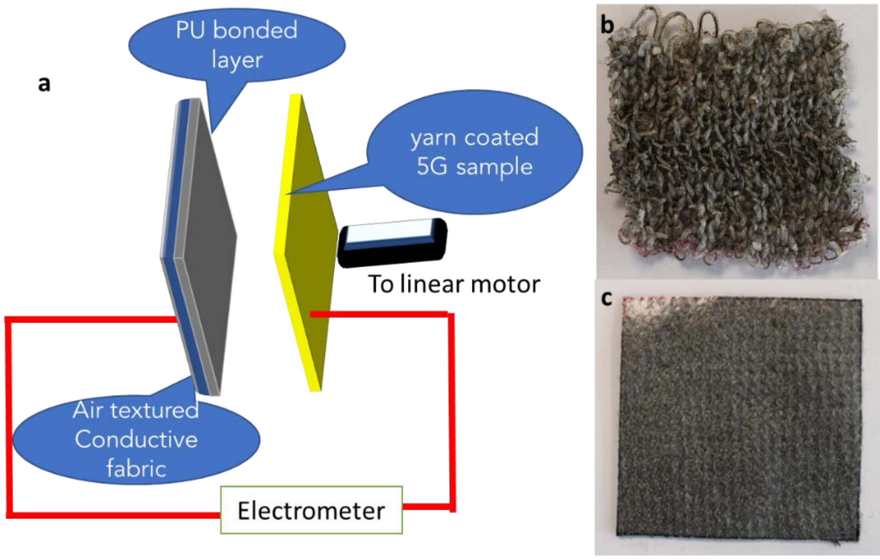

Figure 4.20: Schematic of the a) Final Prototype, b) 5G Knitted Sample, c) Air Textured PU Bonded Sample.

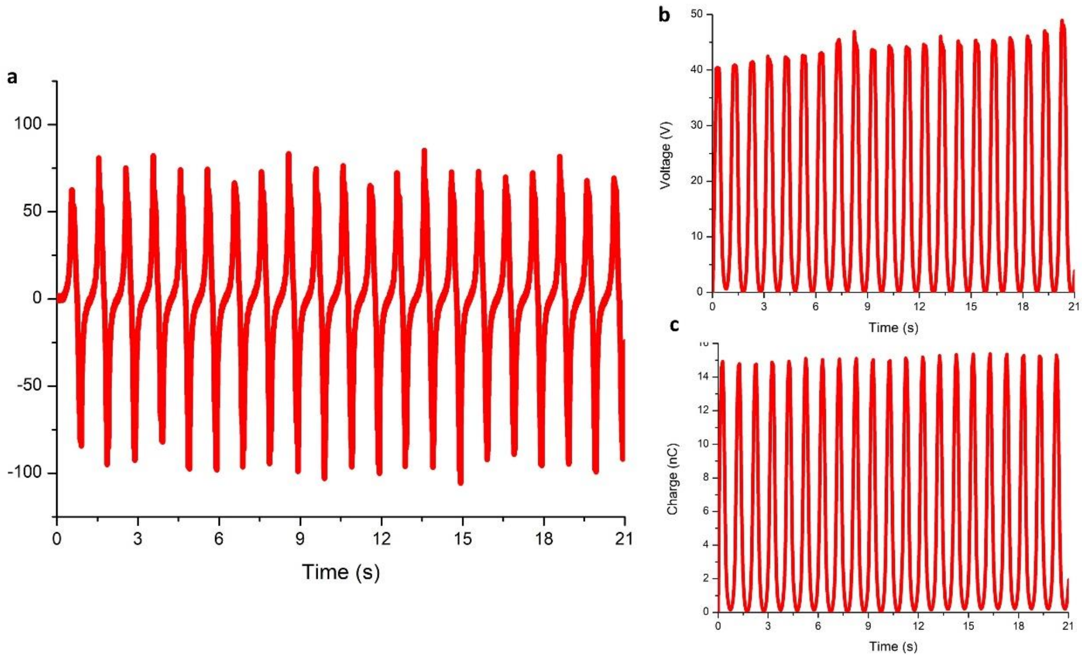

Figure 4.21: Electrical Characterization Between PDMS Yarn Coated Sample and Air Textured PU Bonded Sample (a) Short Circuit Current, (b) Open Circuit Voltage (c) Open Circuit Charge.

All previous samples were tested against a 5G knitted PU coated sample, and for this experiment, silver-coated nylon yarn was air textured before knitting. After preparation, as given in Figure 4.20a, schematic prepared and testing were performed.

Air texturing further opens the fibres in the yarn and thus enhance the surface area of the yarn.

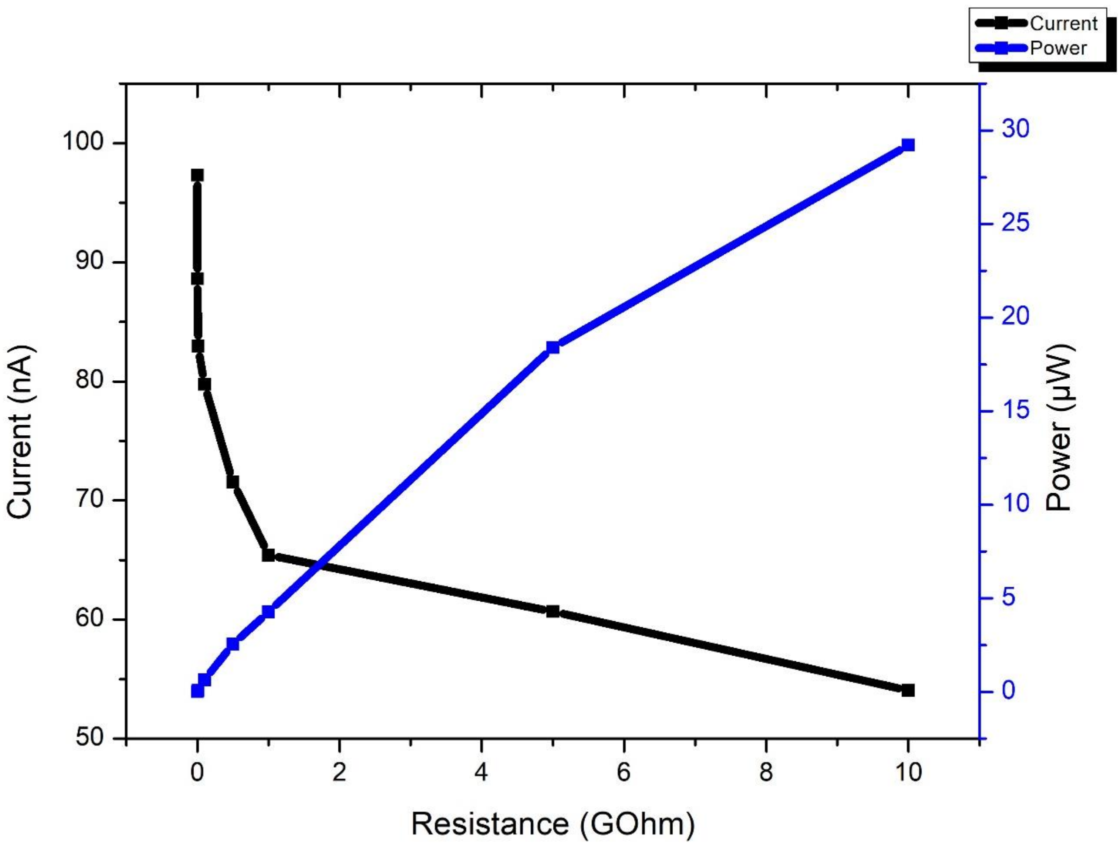

Figure 4.22: Current and Power Through Different Resistors Attached to the Final TENG Device.

As shown in Figure 4.21, the final prototype could exhibit a maximum short circuit current of 85.3 nA, a charge density of 6.12 μC/m^{2}and a maximum open-circuit voltage of 51.08 V under the 1 mm amplitude over 1 Hz frequency. To analyze the power generation of the final TENG device, a series of resistors and the current flow through the circuit were measured. According to Figure 4.22, the final prototype could generate a peak power of 116.8 mW/m^2 through 10 GΩ resistors under the same motion profile.

4.4. Textile Properties of TENG Layer Application Techniques

Textile testing is one of the crucial analysis related to this research project. In our previous works, we have presented when using printing dip coating methods can compromise most of the TENG devices' textile-related properties [1]. In case to verify the estimation, here selected textile testing was carried out.

4.4.1. Air permeability test results

Air permeability is defined as the flow rate of pressurised air through the test subject in the vertical direction. Based on the end, product comfort-related properties are the tendency to changed. Moreover, measuring the properties under standard testing method suitable product can be finalized[59] (Figure 4.23).

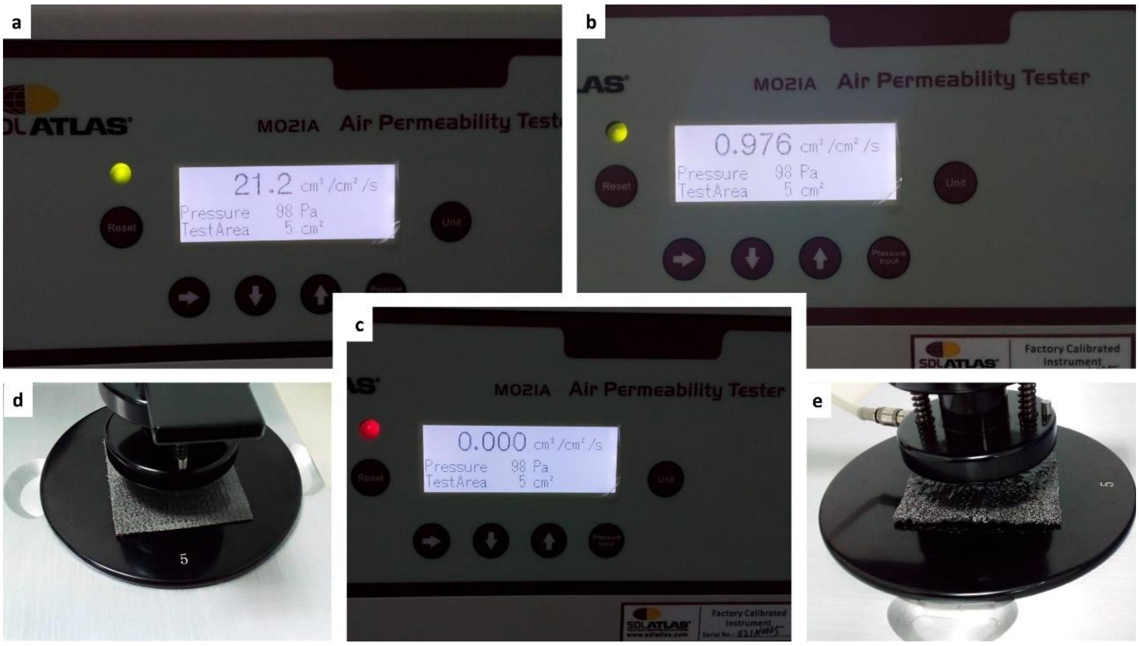

Figure 4.23: Air Permeability Result for a) Silicone Printed Sample, b) PU Bonded Sample, c) Air Permeability Test Initialization State, Samples set up d) PU Bonded Sample, e) Silicone Printed Sample

Dip coated and PU bonded sample shows very low air permeability while the yarn-coated sample shows very high air permeability. Silicone printed sample shows moderate air permeability under the 98 Pa testing pressure. The dip-coated sample's pores and PU bonded surfaces have completely covered with Silicone and PU; thus, air could not penetrate the samples. In that scenario, the air permeability of dip-coated and PU samples has appeared at very minimum values (Table 4.4).

Table 4.4: Air Permeability Test Results

Sample	**Result ($cm^3/cm^2/s$)**
N1	0.551
PU bonded	0.904
N2	21.2
N3	101

However, enough spaces are available in the fabric for air to permeate to the other side in the yarn coated knitted sample. Thus, it confirmed that the yarn coating sample had the highest air permeability compared with all different samples. If the end product will be outdoor clothing, it is advisable to use low air permeable fabrics that enable protection against wind[60]. When using Yarn coated sample contacted with skin and PU bonded 2^{nd} electrode on top of that while contact and separation, the device can exhibit the required air permeability characteristics. If the final device needs to enhance air permeability further, the PU bonded sample needs to be replaced with a PU yarn coated sample.

4.4.2. Moisture management test result

Wetting time– This is a direct reading given by the moisture management tester. This was defined as the time in seconds when the slope of total water content at the top and bottom surface becomes more significant than tan (150^0), respectively. The top surface had fast wetting in the dip-coated sample, and the bottom surface had no wetting (Table 4.5). This was because of the complete coverage of the sample by silicon and no pores for moisture to penetrate from one surface to another. When the printed side was taken as the top surface, there was a medium-wetting time, while the bottom had a very fast wetting time for a printed sample. There were small pores on the surface that provided interconnected paths to move from one surface to another. The silver-coated yarn had an affinity towards moisture, and thus it has worked as a hydrophilic surface compared with the silicone-coated top surface. Even when the printed sample's uncoated surface was taken into the top surface, it has wetted very fast, and there is no wetting on the other side at that time. In yarn coated sample, both surfaces had shown very fast wetting. The main reason is the knitting structure that has allowed for high wicking, and the porous structure has given enough space for moisture transmission from one surface to another.

The secondary electrode was covered with a PU bonding layer with 102 microns, including a 51-micron adhesive part. When applying recommended heat and pressure, the sticky part melted and bonded between the fabric and the outer PU layer. Since the fabric layer is not uniform due to the air texturing effect and the knitting structure, a micro-scale opens on top of several yarns. According to moisture wetting time results, the upper surface takes 1.219 s while the bottom takes 11.344 s. This happens due to the fabric substrate's moisture-wicking behaviour. One possibility for this result is that PU is an initially hydrophobic material, but since there are open channels in the top surface, water has made channels through that. That makes the bottom surface also wetted after the given period.

Absorption rate (Table 4.5)– Absorption rate is the average moisture absorption ability of the fabric top and bottom surfaces in the water inlet pump time, respectively. Dip coated sample had a medium absorption rate. The printed side top sample had a fast absorption rate, the printed side upside down had a slow absorption rate, and the yarn coated sample showed high absorbency.

Surface modifications of PU bonded, dip-coated and printed samples was acted as a barrier for the absorption. Instead of absorbing the fabric, the moisture has wetted the surface and shows some value for the samples' absorbance. In the yarn coating sample, since there were free spaces available due to capillary action, moisture can move along the surface. According to gong et al. [61], moisture absorption characteristics of silicone rubber concluded that moisture diffusion behaviour of Silicone is tally with Fick’s law (rate of diffusion will increase with the surface area and concentration difference of the given silicone coating sample and when increasing the thickness rate of diffusion reduces). The high moisture absorbency can lead to the reduction of dielectric properties. This is a negative point related to the usage of Silicone for TENG applications.

Even in PU bonded sample, after the moisture moved to the electrode surface, it can create charge collection problems. It is favourable to use the PU yarn coating method for future developments along with higher thickness to reduce the penetration. But thickness needs to be prudently analysed since more increased thickness can lead to lower electrical charge induction.

Max wetting circle, spreading speed (Table 4.5)- Max wetting cycle and spreading speed purely depend on the samples' wicking properties and capillary action. The dip-coating sample had shown no wetting, while the printed side top sample had shown no wetting of the top surface. Because of low adhesive and cohesive forces was resulted from the less intermolecular interconnection between Silicone and water, the wettability, wetting circle and spreading were very law in completely Silicone coated samples. When the top surface was a silver-coated nylon knitted structure, there was high wettability, maximum wetting circle, and breakneck wetting speed because of the silver-coated nylon yarn's affinity towards moisture. Yarn coated with silicone sample also showed max wetting circle and very fast spreading speed for both surfaces due to the knitting structural advancement.

The secondary PU coated electrode upper surface had a 25 mm wetting circle, while the lower surface had a 15 mm wetting circle. The top surface wetting circle purely based on the hydrophobic nature of the PU bonded layer. Water had moved on top of the surface once it increases with time. On the other hand, after water vertically travelled to the lower surface, the same action happened as silicone printed samples.

One-way transport capability (Table 4.5) - Since the dip-coated sample is hydrophobic, there was no moisture transport between surfaces. The printed sample has shown some transportation because of the pores in the structure. But the number of pores on the surface was meagre. Moreover, PU bonded samples had better moisture transportation capability with the channels made by the air texturing effect and the bonding behaviour. In yarn coated sample, it has shown very fast one-way transport capability because of the pores structure.

Under these factors, the dip-coated sample can be categorized as a waterproof fabric. The printed side was taken into the top side had medium moisture management properties, printed side upside bottom had waterproof behaviour, and yarn coated sample and PU bonded sample had good moisture management properties (Figure 4.24).

Table 4.5: Summarization of Moisture Management Test Results for All Samples

sample	Parameter	Top surface	Bottom surface
N1	Wetting time	3.563 s	120 s (no wetting)
	Absorption rate	30.4192% s^{-1}	-
	Max wetting radius	5 mm	-
	Spreading speed	1.33 mm/s	
	One-way transport capability	-618.8963	
N2 printed side top	Wetting time	6.75s	1.219s
	Absorption rate	52.6082% s^{-1}	4.2663% s^{-1}
	Max wetting radius	5 mm	30 mm
	Spreading speed	0.7208 mm/s	4.9169 mm/s
	One-way transport capability	3238.0903	
N2 printed side upside bottom	Wetting time	0.187 s	120 s
	Absorption rate	3.4912% s^{-1}	-
	Max wetting radius	30 mm	-
	Spreading speed	7.2347	0
	One-way transport capability	-4097.0181	
N3	Wetting time	0.187 s	0.187 s
	Absorption rate	52.7074% s^{-1}	9.1655% s^{-1}
	Max wetting radius	30 mm	30 mm
	Spreading speed	4.0692 mm/s	21.0834 mm/s
	One-way transport capability	785.6304	
PU bonded sample	Wetting time	1.219 s	11.344 s
	Absorption rate	130.1472% s^{-1}	7.4177% s^{-1}
	Max wetting radius	25 cm	15 cm
	Spreading speed	4.7545 mm/s	2.0983 mm/s
	One-way transport capability	578.6887	

Index	Grade	1	2	3	4	5
Wetting time	Top	≥ 120 No wetting	20–119 Slow	5–19 Medium	3–5 Fast	< 3 Very fast
	Bottom	≥120 No wetting	20–119 Slow	5–19 Medium	3–5 Fast	<3 Very fast
Absorption rate	Top	0–10 Very slow	10–30 Slow	30–50 Medium	50–100 Fast	> 100 Very fast
	Bottom	0–10 Very slow	10–30 Slow	30–30 Medium	50–100 Fast	>100 Very fast
Maximum wetted radius	Top	0–7 No wetting	7–12 Slow	12–17 Medium	17–22 Large	> 22 Very large
	Bottom	0–7 No wetting	7–12 Slow	12–17 Medium	17–22 Large	>22 Very large
Spreading speed	Top	0–1 Very slow	1–2 Slow	2–3 Medium	3–4 Fast	> 4 Very fast
	Bottom	0–1 Very slow	1–2 Slow	2–3 Medium	3–4 Fast	>4 Very fast
One way transport capacity	<−50		− 50 to 100	100–200	200–400	> 400
	Poor		Fair	Good	Very good	Excellent
Overall moisture management	0–0.2		0.2–0.4	0.4–0.6	0.6–0.8	> 0.8
	Poor		Fair	Good	Very good	Excellent

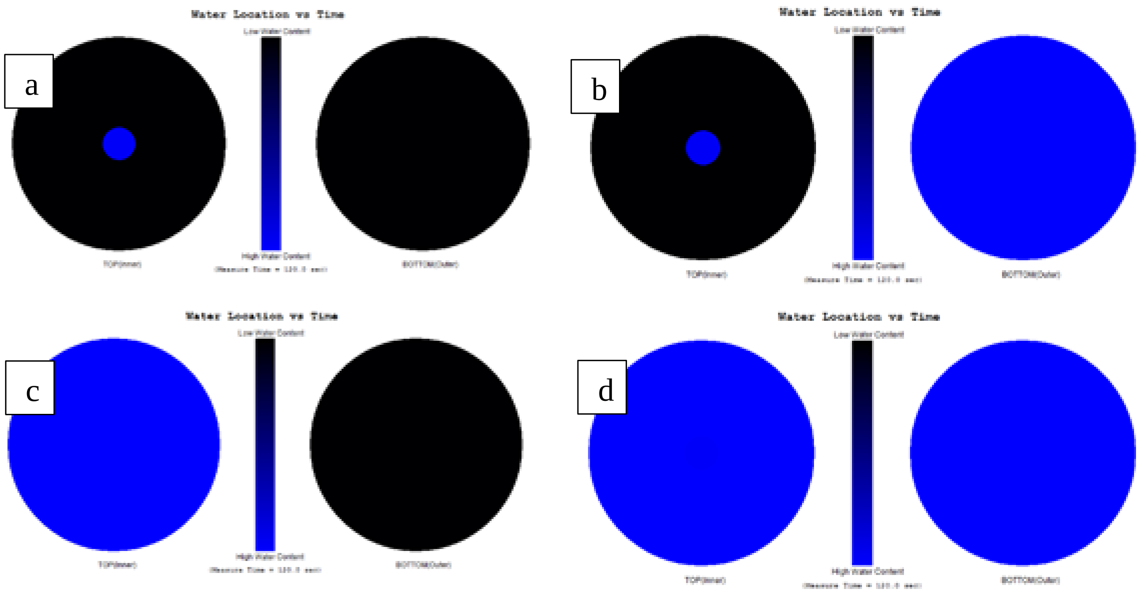

Figure 4.24: water location vs time for a) Dip Coated, b) Printed Sample Printed Side Top, c) Printed Sample Unprinted Side Top, d) Yarn Coated and PU Bonded Samples

4.4.3. Stretch and recovery test results.

According to stretch and recovery test results for the primary electrode and triboelectric surface, the yarn coated knitted structure exhibited the highest stretchability. Simultaneously, the printed sample has shown medium stretchability, and the dip-coated sample (Figure 4.25)has shown the lowest stretchability (Table 4.6). However, the dip-coated sample demonstrated the highest recoverability, followed by the printed sample and the yarn coated sample (Table 4.6). Even though all samples were prepared using a knitted structure, in the dip-coated sample after the fabric was covered entirely by Silicone, the outer coating completely governed the incorporated fabric properties. Since the layer was prepared 1.3491mm thick compared with the thickness of the fabric, most of the stretch and recovery properties were based on the coating itself. Even in the printed structure, mechanical properties are governed by the silicone coating to some extent. In yarn coated construction, knitted loops have extra space to move on each other. Because of that, the structure could withhold higher stretchability but lower recovery properties. By comparing each sample's modulus, we can conclude that the yarn coated sample was more sensitive for a given force. It always undergoes mechanical deformation under little pressure inclined onto that. This is an important parameter since the yarn coated knitted structure is vital for TENG development as a self-powered sensor.

When looking into the PU bonded secondary electrode sample's stretch and recovery value, that also exhibits excellent results along with the yarn coated sample. Furthermore, this sample shows a high elastic modulus that enables the final compact prototype to withstand high pressure during human movements. Even though stretchability is higher for Silicone yarn coated sample and PU bonded selection, both exhibits lower recoverability properties.

Table 4.6: Summarization of the Stretch and Recovery Results

Sample	**Max stretch**	**Stretchability**	**Recoverability**	**Elastic modulus (MPa)**
N1	56.99 mm	12.18%	100%	1.8185
N2	68.205 mm	34.26%	97.5%	1.651
N3	89.32 mm	75.82%	76.67%	1.4093
PU bonded fabric	80.725 mm	58.9%	69.28 %	4.5123

A comparison of the tensile behaviour of uncoated yarn sample and coated yarn sample results are summarized below (Table 4.7) (Figure 4.27). According to the results, there was a slight increase in the sample's stress and strain, and when the yarn is coated, the modulus has reduced. This is a negative point when using this as a self-powered sensing device. By using the knitted structure to prepare the TENG, the effect of this has been reduced.

Table 4.7: Summarization of Tensile Behaviour of Coated and Uncoated Yarn

Sample	**Max displacement**	**Max load**	**Elastic modulus**
Uncoated sample (Figure 4.26)	92.50mm	18.68N	0.1225N/tex
Coated sample (Figure 4.27: Tensile Test for Coated Sample)	92.91mm	19.43N	0.0632N/tex

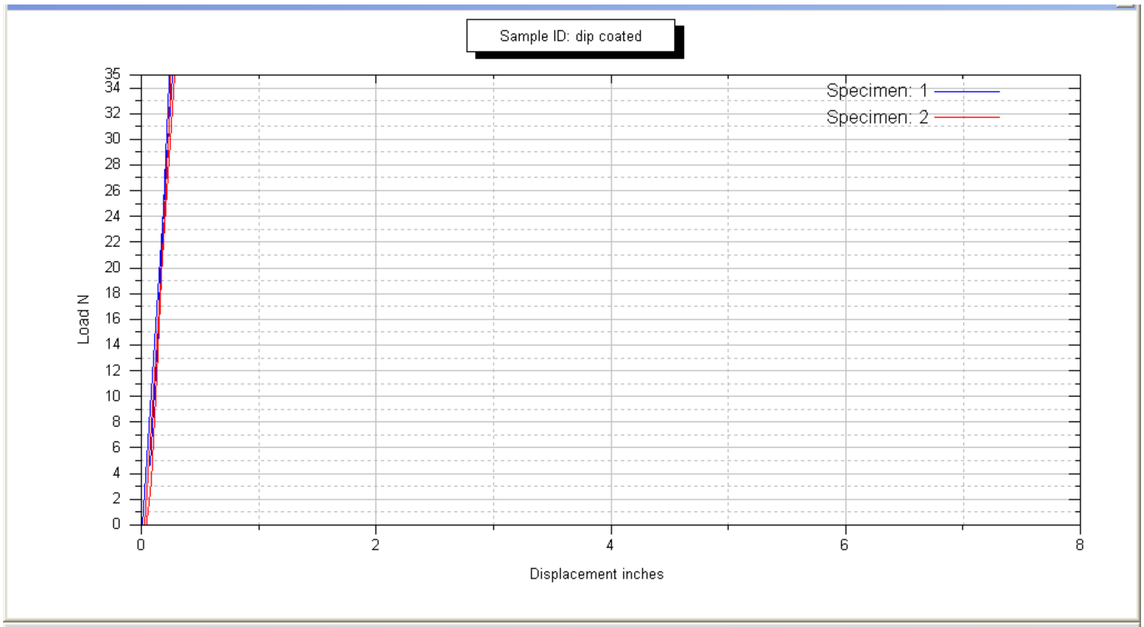

Test Results

Sp No	MAX.LOAD (N)	MAX.DISP (mm)	LOAD.PSP1 (N)	LOAD.PSP2 (N)	LOAD.PSP3 (N)	LOAD.PSP4 (N)	MODULUS (MPa)
1	35.97	6.150	--------	--------	--------	--------	1.835
2	34.49	6.230	--------	--------	--------	--------	1.802

Figure 4.25: Stretch and Recovery Test for Dip-coated Sample.

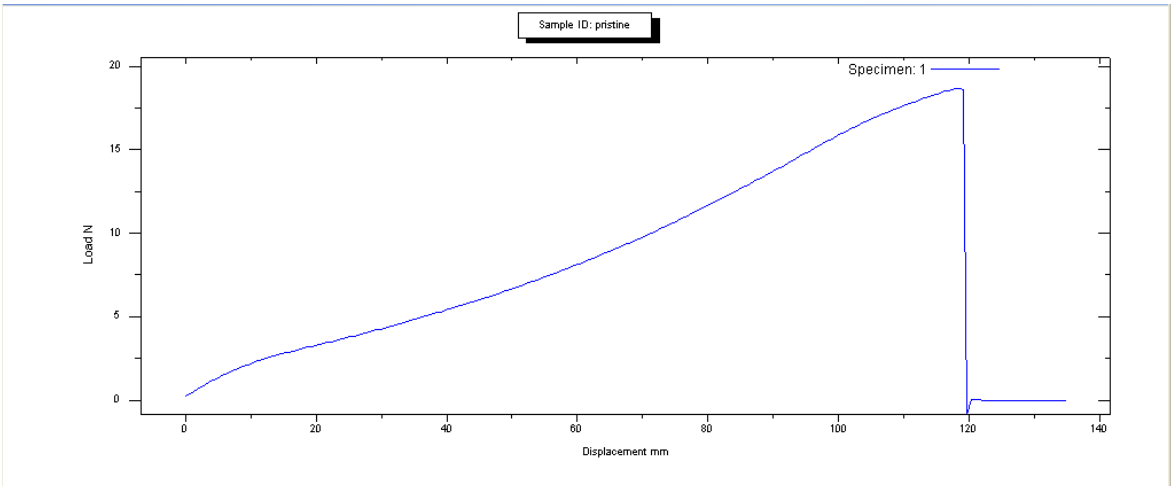

Test Results

Sp No	MAX.DISP (mm)	MAX.LOAD (N)	%STN.MAX (%)	MAX.TEN (N/tex)	MODULUS (N/tex)
1	92.50	18.68	217.8	0.2135	0.1225

Figure 4.26: Tensile Test for Uncoated Sample

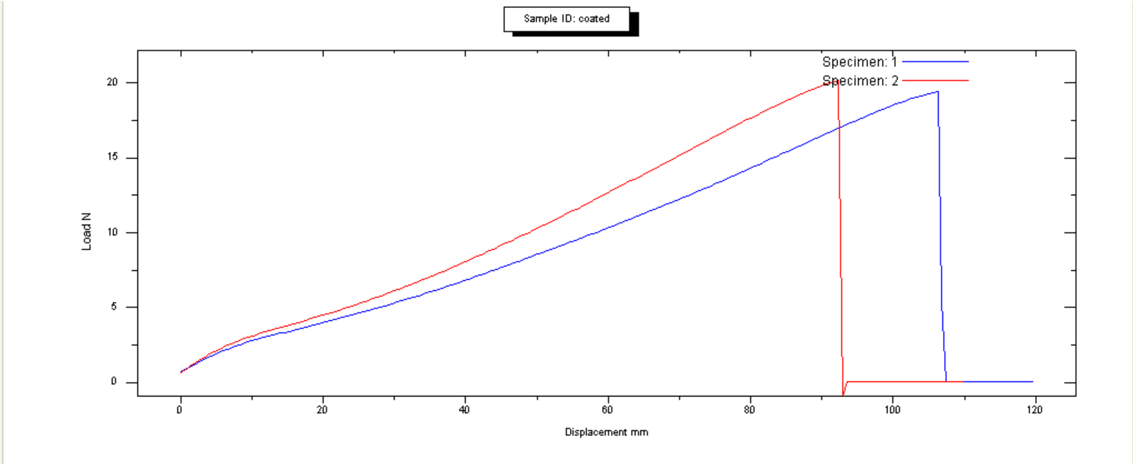

Test Results

Sp No	MAX.DISP (mm)	MAX.LOAD (N)	%STN.MAX (%)	MAX.TEN (N/tex)	MODULUS (N/tex)
1	92.91	19.43	212.6	0.1143	0.0632
2	82.67	20.18	200.3	0.1187	0.0739

Figure 4.27: Tensile Test for Coated Sample

CHAPTER 5

5. CONCLUSION AND RECOMMENDATIONS

5.1. Key Conclusion

The proposed research aims to develop a coated yarn-based TENG device with wearable textile properties. This report highlighted the project's progress in a literature survey, material selection, yarn coating development, analysis of the performance of yarn coating system against the screen-printing and dip coating methods, and the use of air texturing technique to enhance the results further. Experiments have been conducted to investigate parameters, which could influence the TENG behaviour. The result of SEM images, open-circuit voltage, close-circuit current, open circuit charge density, maximum power output under different resistors, final microscopic images, textile testing results on air permeability, moisture management property and stretch and recovery shows the possibility of an improved yarn coating system for silver-coated nylon yarn to fabricate TENG devices in mass scale.

Silicone yarn coated sample show better and even coverage, good air permeability (101 $cm^3/cm^2/s$), high moisture management properties and high stretchability (Stretchability -75.82 %, Recoverability- 76.67% and elastic modulus of 1.4093). There are adverse effects such as low recoverability due to the structure and controlled when using a substrate.

Furthermore, when the PDMS yarn coated sample was subjected to contact separation motion with PU bonded conductive fabric with 1 mm amplitude under 1 Hz frequency, it could generate a maximum short circuit current of 60.10 nA, 13.8 $\mu C/m^2$ Charge density and 34.53 V close circuit voltage.

After finding this result to enhance the device's power output further, the secondary triboelectric layer and electrode were changed. The electrode substrate was first air textured and then knitted using a gauge five flatbed knitting machine. Previously used PU coating was used as the triboelectric layer for this experiment. The secondary electrode exhibits moisture management properties and high stretchability (Stretchability -58.9 %, Recoverability- 69.28% and elastic modulus of 4.5123 MPa) with no air permeability.

The final prototype could generate the maximum short circuit current of 85.3 nA, the charge density of 6.12 μC/m^2 and maximum open-circuit voltage of 51.08 V under the 1 mm amplitude over 1 Hz frequency. Finally, the device used to generate a peak power of 0.1168 mW/m^2 through 10 GΩ resistors under the same motion profile.

5.2. Recommendations

Since TENG devices are susceptible to moisture and temperature, it is essential to maintain specific standard figures for temperature and humidity while operating with this device. Moreover, it is advisable to place the device in many possible positions (Figure 5.1) on the body to maximize the power output and absolute consistency.

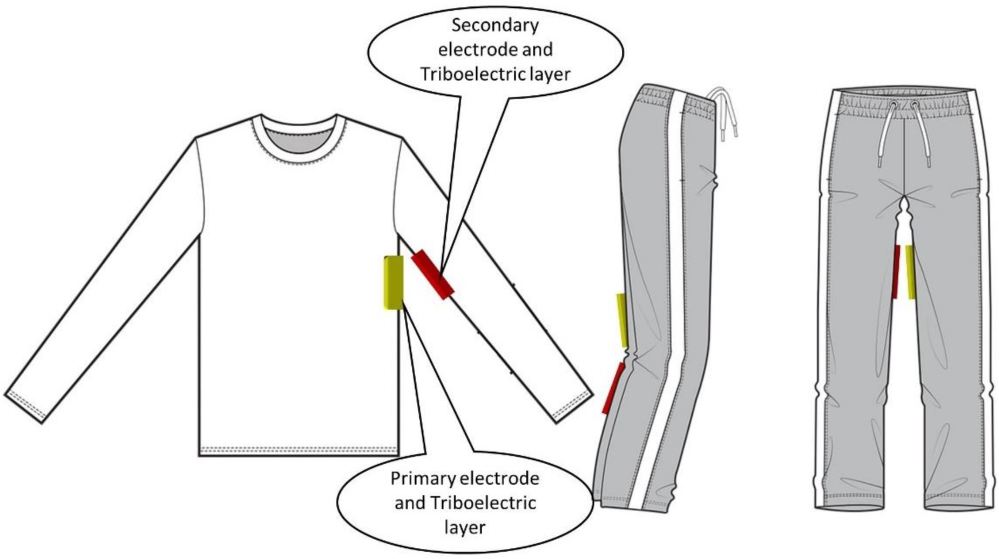

Figure 5.1: Places on Garments to Place the Developed TENG Device

Publications from this project

K. R. S. D. Gunawardhana, N. D. Wanasekara, and R. D. I. G. Dharmasena, “Towards Truly Wearable Systems: Optimizing and Scaling Up Wearable Triboelectric Nanogenerators,” *iScience*, vol. 23, no. 8, p. 101360, 2020.

Reference

[1] K. R. S. D. Gunawardhana, N. D. Wanasekara, and R. D. I. G. Dharmasena, "Towards Truly Wearable Systems: Optimizing and Scaling Up Wearable Triboelectric Nanogenerators," *iScience*, vol. 23, no. 8, p. 101360, 2020.

[2] R. D. I. G. Dharmasena and S. R. P. Silva, "Towards optimized triboelectric nanogenerators," *Nano Energy*, vol. 62, pp. 530–549, 2019.

[3] A. Satharasinghe, T. Hughes-Riley, and T. Dias, "A review of solar energy harvesting electronic textiles," *Sensors (Switzerland)*, vol. 20, no. 20, pp. 1–39, 2020.

[4] T. Huang *et al.*, "Fabric texture design for boosting the performance of a knitted washable textile triboelectric nanogenerator as wearable power," *Nano Energy*, vol. 58, no. December 2018, pp. 375–383, Apr. 2019.

[5] C. Chen *et al.*, "Direct Current Fabric Triboelectric Nanogenerator for Biomotion Energy Harvesting," *ACS Nano*, vol. 14, no. 4, pp. 4585–4594, Apr. 2020.

[6] S. S. Kwak, H. Kim, W. Seung, J. Kim, R. Hinchet, and S.-W. Kim, "Fully Stretchable Textile Triboelectric Nanogenerator with Knitted Fabric Structures," *ACS Nano*, vol. 11, no. 11, pp. 10733–10741, Nov. 2017.

[7] D. J. Spencer, *Knitting technology : a comprehensive handbook and practical guide*, 1st ed. CRC Press, 2001.

[8] V. Nguyen, R. Zhu, and R. Yang, "Environmental effects on nanogenerators," *Nano Energy*, vol. 14, pp. 49–61, 2014.

[9] W. Paosangthong, R. Torah, and S. Beeby, "Recent progress on textile-based triboelectric nanogenerators," *Nano Energy*, vol. 55, no. August 2018, pp. 401–423, 2019.

[10] Z. L. Wang, J. Chen, and L. Lin, "Progress in triboelectric nanogenerators as a new energy technology and self-powered sensors," *Energy Environ. Sci.*, vol. 8, no. 8, pp. 2250–2282, 2015.

[11] S. Liu, W. Zheng, B. Yang, and X. Tao, "Triboelectric charge density of porous and deformable fabrics made from polymer fibers," *Nano Energy*, vol. 53, pp. 383–390, 2018.

[12] H. Zou *et al.*, "Quantifying the triboelectric series," *Nat. Commun.*, vol. 10, no. 1, pp. 1–9, 2019.

[13] Z. L. Wang, “Triboelectric nanogenerators as new energy technology and self-powered sensors - Principles, problems and perspectives,” *Faraday Discuss.*, vol. 176, no. 0, pp. 447–458, 2014.

[14] T. T. Nanogenerator *et al.*, “Topographically-Designed Triboelectric Nanogenerator via Block Copolymer Self-Assembly,” *Nano Lett.*, vol. 14, no. 12, pp. 7031–7038, 2014.

[15] L. Lin *et al.*, “Segmentally structured disk triboelectric nanogenerator for harvesting rotational mechanical energy,” *Nano Lett.*, vol. 13, no. 6, pp. 2916–2923, 2013.

[16] S. Wang, L. Lin, Y. Xie, Q. Jing, S. Niu, and Z. L. Wang, “Sliding-triboelectric nanogenerators based on in-plane charge-separation mechanism,” *Nano Lett.*, vol. 13, no. 5, pp. 2226–2233, 2013.

[17] P. Bai *et al.*, “Cylindrical Rotating Triboelectric,” *ACS Nano*, vol. 7, no. 7, pp. 6361–6366, 2013.

[18] R. D. I. G. Dharmasena, J. H. B. Deane, and S. R. P. Silva, “Nature of Power Generation and Output Optimization Criteria for Triboelectric Nanogenerators,” *Adv. Energy Mater.*, vol. 8, no. 31, pp. 1–11, 2018.

[19] J. Chen, H. Guo, X. Pu, X. Wang, Y. Xi, and C. Hu, “Traditional weaving craft for one-piece self-charging power textile for wearable electronics,” *Nano Energy*, vol. 50, pp. 536–543, 2018.

[20] C. Ning *et al.*, “Washable textile-structured single-electrode triboelectric nanogenerator for self-powered wearable electronics,” *J. Mater. Chem. A*, vol. 6, no. 39, pp. 19143–19150, 2018.

[21] W. Gong *et al.*, “A wearable, fibroid, self-powered active kinematic sensor based on stretchable sheath-core structural triboelectric fibers,” *Nano Energy*, vol. 39, pp. 673–683, 2017.

[22] F. He *et al.*, “Stretchable, Biocompatible, and Multifunctional Silk Fibroin-Based Hydrogels toward Wearable Strain/Pressure Sensors and Triboelectric Nanogenerators,” *ACS Appl. Mater. Interfaces*, vol. 12, no. 5, pp. 6442–6450, 2020.

[23] K. Dong *et al.*, “3D Orthogonal Woven Triboelectric Nanogenerator for Effective Biomechanical Energy Harvesting and as Self-Powered Active Motion Sensors,”

Adv. Mater., vol. 29, no. 38, pp. 1–11, 2017.

[24] J. Xiong *et al.*, "Skin-touch-actuated textile-based triboelectric nanogenerator with black phosphorus for durable biomechanical energy harvesting," *Nat. Commun.*, vol. 9, no. 1, pp. 1–9, 2018.

[25] L. Zhang *et al.*, "All-Textile Triboelectric Generator Compatible with Traditional Textile Process," *Adv. Mater. Technol.*, vol. 1, no. 9, p. 1600147, Dec. 2016.

[26] Y. T. Jao *et al.*, "A textile-based triboelectric nanogenerator with humidity-resistant output characteristic and its applications in self-powered healthcare sensors," *Nano Energy*, vol. 50, pp. 513–520, 2018.

[27] R. Pan *et al.*, "Fully biodegradable triboelectric nanogenerators based on electrospun polylactic acid and nanostructured gelatin films," *Nano Energy*, vol. 45, no. December 2017, pp. 193–202, 2018.

[28] K. Dong *et al.*, "A Highly Stretchable and Washable All-Yarn-Based Self-Charging Knitting Power Textile Composed of Fiber Triboelectric Nanogenerators and Supercapacitors," *ACS Nano*, vol. 11, no. 9, pp. 9490–9499, 2017.

[29] J. Lee *et al.*, "Conductive fiber-based ultrasensitive textile pressure sensor for wearable electronics," *Adv. Mater.*, vol. 27, no. 15, pp. 2433–2439, 2015.

[30] Y.-C. Lai, J. Deng, S. L. Zhang, S. Niu, H. Guo, and Z. L. Wang, "Single-Thread-Based Wearable and Highly Stretchable Triboelectric Nanogenerators and Their Applications in Cloth-Based Self-Powered Human-Interactive and Biomedical Sensing," *Adv. Funct. Mater.*, vol. 27, no. 1, p. 1604462, Jan. 2017.

[31] Y. Cheng *et al.*, "A stretchable fiber nanogenerator for versatile mechanical energy harvesting and self-powered full-range personal healthcare monitoring," *Nano Energy*, vol. 41, pp. 511–518, 2017.

[32] Y. Guo *et al.*, "All-fiber hybrid piezoelectric-enhanced triboelectric nanogenerator for wearable gesture monitoring," *Nano Energy*, vol. 48, pp. 152–160, 2018.

[33] X. S. Zhang, M. Han, B. Kim, J. F. Bao, J. Brugger, and H. Zhang, "All-in-one self-powered flexible microsystems based on triboelectric nanogenerators," *Nano Energy*, vol. 47. Elsevier Ltd, pp. 410–426, 01-May-2018.

[34] X. He *et al.*, "A Highly Stretchable Fiber-Based Triboelectric Nanogenerator for Self-Powered Wearable Electronics," *Adv. Funct. Mater.*, vol. 27, no. 4, pp. 1–8, 2017.

[35] F. Invernizzi, S. Dulio, M. Patrini, G. Guizzetti, and P. Mustarelli, “Energy harvesting from human motion: Materials and techniques,” *Chemical Society Reviews*, vol. 45, no. 20. Royal Society of Chemistry, pp. 5455–5473, 21-Oct-2016.

[36] W. Seung *et al.*, “Nanopatterned textile-based wearable triboelectric nanogenerator,” *ACS Nano*, vol. 9, no. 4, pp. 3501–3509, 2015.

[37] B. Dudem, A. R. Mule, H. R. Patnam, and J. S. Yu, “Wearable and durable triboelectric nanogenerators via polyaniline coated cotton textiles as a movement sensor and self-powered system,” *Nano Energy*, vol. 55, pp. 305–315, 2019.

[38] J. Zhou *et al.*, “Fiber-Based Generator for Wearable Electronics and Mobile Medication,” *ACS Nano*, vol. 8, no. 6, pp. 6273–6280, 2014.

[39] T. Zhou, C. Zhang, C. B. Han, F. R. Fan, W. Tang, and Z. L. Wang, “Woven Structured Triboelectric Nanogenerator for Wearable Devices,” *ACS Appl. Mater. Interfaces*, vol. 6, no. 16, pp. 14695–14701, Aug. 2014.

[40] M. Lou *et al.*, “Highly Wearable, Breathable, and Washable Sensing Textile for Human Motion and Pulse Monitoring,” *ACS Appl. Mater. Interfaces*, vol. 12, no. 17, pp. 19965–19973, Apr. 2020.

[41] C. Ye, S. Dong, J. Ren, and S. Ling, “Ultrastable and High-Performance Silk Energy Harvesting Textiles,” *Nano-Micro Lett.*, vol. 12, no. 1, pp. 1–15, 2020.

[42] Z. Li, M. Zhu, J. Shen, Q. Qiu, J. Yu, and B. Ding, “All-Fiber Structured Electronic Skin with High Elasticity and Breathability,” *Adv. Funct. Mater.*, vol. 30, no. 6, p. 1908411, Feb. 2020.

[43] D. Liu *et al.*, “A constant current triboelectric nanogenerator arising from electrostatic breakdown,” *Sci. Adv.*, vol. 5, no. 4, p. eaav6437, Apr. 2019.

[44] J. Chen *et al.*, “Micro-cable structured textile for simultaneously harvesting solar and mechanical energy,” *Nat. Energy*, vol. 1, no. 10, p. 16138, Oct. 2016.

[45] Q. He *et al.*, “An all-textile triboelectric sensor for wearable teleoperated human–machine interaction,” *J. Mater. Chem. A*, vol. 7, no. 47, pp. 26804–26811, 2019.

[46] M. Sala de Medeiros, D. Chanci, C. Moreno, D. Goswami, and R. V. Martinez, “Waterproof, Breathable, and Antibacterial Self-Powered e-Textiles Based on Omniphobic Triboelectric Nanogenerators,” *Adv. Funct. Mater.*, vol. 29, no. 42, p. 1904350, Oct. 2019.

[47] F. Peng *et al.*, “Facile fabrication of triboelectric nanogenerator based on low-cost thermoplastic polymeric fabrics for large-area energy harvesting and self-powered sensing,” *Nano Energy*, vol. 65, no. July, p. 104068, Nov. 2019.

[48] L. Ma *et al.*, “Continuous and Scalable Manufacture of Hybridized Nano-Micro Triboelectric Yarns for Energy Harvesting and Signal Sensing,” *ACS Nano*, vol. 14, no. 4, pp. 4716–4726, Apr. 2020.

[49] C. Ye, Q. Xu, J. Ren, and S. Ling, “Violin String Inspired Core-Sheath Silk/Steel Yarns for Wearable Triboelectric Nanogenerator Applications,” *Adv. Fiber Mater.*, vol. 2, no. 1, pp. 24–33, Feb. 2020.

[50] L. Zhang *et al.*, “Enhancing the Performance of Textile Triboelectric Nanogenerators with Oblique Microrod Arrays for Wearable Energy Harvesting,” *ACS Appl. Mater. Interfaces*, vol. 11, no. 30, pp. 26824–26829, Jul. 2019.

[51] J. Gong, B. Xu, X. Guan, Y. Chen, S. Li, and J. Feng, “Towards truly wearable energy harvesters with full structural integrity of fiber materials,” *Nano Energy*, vol. 58, no. January, pp. 365–374, Apr. 2019.

[52] W. Fan *et al.*, “Machine-knitted washable sensor array textile for precise epidermal physiological signal monitoring,” *Sci. Adv.*, vol. 6, no. 11, p. eaay2840, Mar. 2020.

[53] X. Pu *et al.*, “A self-charging power unit by integration of a textile triboelectric nanogenerator and a flexible lithium-ion battery for wearable electronics,” *Adv. Mater.*, vol. 27, no. 15, pp. 2472–2478, 2015.

[54] S. Lee *et al.*, “Triboelectric energy harvester based on wearable textile platforms employing various surface morphologies,” *Nano Energy*, vol. 12, pp. 410–418, 2015.

[55] R. D. I. G. Dharmasena *et al.*, “Triboelectric nanogenerators: Providing a fundamental framework,” *Energy Environ. Sci.*, vol. 10, no. 8, pp. 1801–1811, 2017.

[56] R. D. I. G. Dharmasena, K. D. G. I. Jayawardena, C. A. Mills, R. A. Dorey, and S. R. P. Silva, “A unified theoretical model for Triboelectric Nanogenerators,” *Nano Energy*, vol. 48, no. March, pp. 391–400, 2018.

[57] A. Demir, M. Acar, and G. R. Wray, “Air-Jet Textured Yarns: The Effects of Process and Supply Yarn Parameters on the Properties of Textured Yarns,” *Text. Res. J.*, vol. 58, no. 6, pp. 318–328, 1988.

[58] R. D. I. G. Dharmasena, “Inherent asymmetry of the current output in a triboelectric nanogenerator,” *Nano Energy*, vol. 76, p. 105045, Oct. 2020.

[59] V. Kumar, C. Prakash, G. Manigandan, and V. R. Sampath, “Investigation of the influence of stretch on the air permeability of knitted fabric: Effect of loop length,” *Fibres Text. East. Eur.*, vol. 29, no. 1, pp. 53–56, 2021.

[60] F. Selli and Y. Turhan, “Investigation of Air Permeability and Moisture Management Properties of the Commercial Single Jersey and Rib Knitted FabricTicari Süprem VeRibana Örme Kumaşlarin HaGeçirgenliği Ve NeYönetimÖzelliklerinin Araştirilmasi,” *TEKSTİL ve KONFEKSİYON*, vol. 27, no. 1, p. 2017, 2017.

[61] W. Gong *et al.*, “Continuous and scalable manufacture of amphibious energy yarns and textiles,” *Nat. Commun.*, vol. 10, no. 1, p. 868, Dec. 2019.